“Real Time Image Transmission using FPGA on WARP test bed”

Thesis submitted in the partial fulfillment of requirement

for the award of degree of

Master of Engineering

In

Electronics and Communication Engineering

Submitted by:

Ruchi Verma

801061031

Under the guidance of:

Dr.Rajesh Khanna

Professor, ECED

ELECTRONICS AND COMMUNICATION ENGINEERING DEPARTMENT

THAPAR UNIVERSITY

(Established under the section 3 of UGC Act, 1956)

PATIALA – 147004 (PUNJAB)

CERTIFICATE

I, "**Ruchi Verma**", hereby certify that the work which is being presented in this thesis entitled "**Real Time Image Transmission using FPGA on WARP test bed**" by me in partial fulfillment of the requirements for the award of degree of Master of Engineering in Electronics and Communication Engineering from Thapar University (Deemed University), Patiala, is an authentic record of my own work carried out under the supervision of "**Dr.Rajesh khanna**".

The matter presented in this thesis has not been submitted in any other University/Institute for the award of any other degree.

Ruchi

(Signature of student)
Ruchi Verma
801061031

Date: 27 June 2012

It is certified that the above statement made by the student is correct to the best of my knowledge and belief.

Dr.Rajesh Khanna
Professor, ECED

Date: 27 June 2012

Counter signed by:

(Dr. Rajesh Khanna)
Professor and Head ECED
Thapar University, Patiala
Date:

(Dr. S.K. Mohapatra)
Dean of Academic Affairs
Thapar University, Patiala
Date:

ACKNOWLEDGEMENT

A good job is never the outcome of the efforts of a single person. I feel myself lucky to express my profound sense of gratitude and respect to all those who helped me directly or indirectly throughout my thesis.

I would like to give special thanks to my guide **Dr.Rajesh Khanna,** Professor **ECED**, Thapar University, Patiala, for his advice, kind assistance, and invaluable guidance. It has been a great honour to work under him.

I would like to express my deepest gratitude to **Ms.Surbhi Sharma**, Assistant Professor, Electronics and Communication Engineering Department, Thapar University, Patiala, for her advice, motivation, guidance, moral support, efforts and the attitude with which she solved all of my queries in making this report possible.

I would also like to thank all the faculty members of ECED for their intellectual support and also special thanks to my family and my friends who constantly encouraged me to complete this work. I am also thankful to the authors whose work I have consulted and quoted in this work.

Ruchi Verma

801061031

ABSTRACT

The main aim of an effective wireless communication system is to provide a reliable link between the transmitter and the receiver. The wireless link is affected by many factors such as multipath fading, attenuation and shadowing. Due to these reasons a severely attenuated and distorted transmitted signal may arrive at the receiver. This results in a poor signal to noise ratio (SNR), which in turn yields a high bit error rate (BER) at the receiver. There are many solutions to deal with these problems. One solution is the use of channel coding techniques. But this technique involves complex processing and redundancy and hence requires more bandwidth. As a result, channel coding is used with some restrictions. Recent research on *Multiple Input and Multiple Output (MIMO)* systems shows that *STBC* is effective to reduce the fading effect in the wireless channel by providing diversity [41], [42] and this improves BER in receiver. Space–time block coding is a technique used in wireless communications to transmit multiple copies of a data stream across a number of antennas and to exploit the various received versions of the data to improve the reliability of data-transfer.

Alamouti's transmitter diversity scheme is a simplest space time block code technique with support of two transmit antennas and an arbitrary number of receive antennas. The simplest case of Alamouti's Scheme utilizes two transmit antennas and one receive antenna. Alamouti's transmit diversity scheme was the first example of a space-time code which requires only linear pre processing at receiver. The scheme has been implemented in many research papers but most of the results are presented through simulations. In this thesis the Alamouti scheme has been implemented on a WARP test board. The proposed system of Alamouti STBC transmits grey scale image through wireless channel in real time scenario on a WARP test bed. WARP is Wireless Access Research Platform.

In this thesis we have implemented a MIMO communication system on WARP test bed which has a FPGA (VIRTEX IV) processor. We are using FPGA because it gives faster output than DSP processor. So if we are implementing receiver which has more complexity than Transmitter on FPGA then it will give results faster than DSP. We have implemented Alamouti STBC for different modulation schemes and with different number of transmitting and receiving antennas. Also using Alamouti STBC for different number of transmitting and receiving antennas Real time transmission of Grey Scale image has also been done using WARP board and different performance metrics are calculated and compared. The WARP board is equipped with four radio cards which are

responsible for processing of signal to be transmitted and received. The signal is modulated by different modulation techniques for their transmission and Bit Error Performance (BER) of these techniques are compared to show best modulation technique amongst all. It can be seen that BER for Binary Phase Shift Keying (BPSK) modulation technique is least but increases as the order of modulation increases.

TABLE OF CONTENTS

LIST OF FIGURES

LIST OF TABLES

LIST OF ABBREVATIONS

ADC	Analog to Digital Converter
AGC	Automatic Gain Control
ASIC	Application Specific Integrated Circuit
AWGN	Additive White Gaussian Noise
BB	Base Band
BER	Bit Error Rate
BPSK	Binary Phase Shift Keying
DAC	Digital to Analog converter
FPGA	Field Programmable Graphical Array
HDL	Hardware Description Language
HF	High Frequency
IEEE	Institute Of Electronics and Electrical Engineers
IF	Intermediate Frequency
ISI	Inter Symbol Interference
MIMO	Multiple Input Multiple Output
MISO	Multiple Input Single Output
M-PSK	M-ary Phase Shift Keying
MRC	Maximal Ratio Combining
OFDM	Orthogonal Frequency Division Multiplexing
PLL	Phase Locked Loop

PSK	Phase Shift Keying
PSNR	Peak Signal To Noise Ratio
QAM	Quadrature Amplitude Modulation
Q-index	Quality Index
QOS	Quality Of Service
QPSK	Quadrature Phase Shift Keying
RF	Radio Frequency
RSSI	Received Signal Strength Indicator
SDR	Software Defined Radio
SER	Symbol Error Rate
SIMO	Single Input Multiple Output
SISO	Single Input Single Output
SNR	Signal to Noise Ratio
STBC	Space Time Block Code
VCO	Voltage Controlled Oscillator
VGA	Variable Gain Amplifier
VHF	Very High Frequency
VLF	Very Low Frequency
WARP	Wireless Open Access Research Platform

CHAPTER 1
INTRODUCTION

1.1 Overview

In the current scenario emphasis is laid more on real time research rather than simulating the system design with software. However one has to simulate in order to determine the basic behaviour but implementing in real time provides correct and actual behaviour of system. The real time implementation can be done on various hardware platform such as software defined radio, WARP FPGA board, ASIC, and DSP based platform. Doing so allows the practical usage of the design and its areas of implementation for the purpose of benefit of society. Further real time system gives opportunity for one to remove or minimize the problems which are encountered practically so that technology given is more reliable and efficient. It is so because the actual conditions responsible for the disruption can be known only in the case of practical and real time systems.

1.2 Real time system

In real time systems the correctness of the system behaviour depends not only on the logical results of the computation, but also on the physical instant at which these results are produced .Real time systems are classified from a number of viewpoints i.e. factors outside the computer system and the factors inside the computer system. A real time system changes its state as a function of physical time. The block diagram of the real time system is shown in figure 1.1 below:

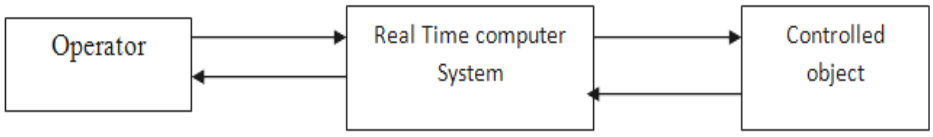

Figure 1.1 Real Time System

A real time system, shown in figure consists of an operator, a human being who operates the overall computer system by giving commands and simulating the design or program responsible for further processing. This computer system is a real time computer system which is controlling the object which is a platform on which design has to be implemented. Thus a real time system depends in both factors i.e. on the factors inside the computer and outside the computer. A real time system can handle a multimedia application for which QoS, CBS algorithm can be employed which uses DWCS to reduce variance in all tasks in real time system. If in a computer system computer utilization is

greater than 1 then CBS algorithm shows good performance, however if the CPU utilization changes then WCCBS algorithm can be used since it has adaptive ability. Further real time system can be classified into broad categories.

1.2.1 Hard Real Time System

Hard real time system are those whose response time is of the order of milliseconds or less and can result in a catastrophe is the conditions are not met [40].The parameters are set and any delay then desired one result in the violation and the system failure occurs. Hard real time systems must remain synchronous with the state of environment in all the cases. Hard real time system is often safety critical.

1.2.2 Soft Real Time System

Soft real time systems are those whose response time is greater higher and not very stringent. Soft real time systems slow down their response time if the load is very high. If an error occurs in soft real time system, the computation is rolled back to the previous established check point to initiate a recovery action. In a soft real time system a critical real time task gets priority over other tasks and retains that priority until it completes.

1.3 Benefits of Real Time System

Firstly real time systems aware all of the value of time. It shows how efficiency can be enhanced if the work is done in desired time. Further wastage of time and resources can be minimized since for progressing, time is the main constraint in today's world. Also automatic tracking of all the processes which are being carried out can be done through real time systems so that any problems if encountered in the work can be removed and analysed at right time. In the research field real time systems play an important role since real time processing generally gives all time slices and system resources to the application or process running in real time. This means that there will be no processing lag caused by the system or other slow applications. Monitoring and controlling of devices can be achieved only when real time systems are employed. Further signal conditioning systems amplifiers, multiplexers, ADC and DAC work in real time. Real time systems reduce cost and physical footprints, sharing of data between different operating systems, make better use of multi core hardware.

- **REDUCED COST AND PHYSICAL FOOTPRINTS**

Multi-OS that makes the use of multiple computers often result in inefficiency. By using the hardware like WARP, you can lower hardware costs while reducing the amount of physical space that your system requires. This is especially important in deployed applications, or in locations where floor space is at premium.

- **SYNCHRONIZATION**

In multiplexing involved in communication like TDM, synchronisation is necessary between transmission and reception. Data from different channels are required to be sent on the same channel with the help of commutator. The data received at destination from channel is de-commutated to individual channel which is done in real time.

- **QUICK PARTITIONING OF RAM AND I/O DEVICES**

Different I/O devices can be partitioned to different operating systems like Lab view and windows n real time according to supported configurations. Partitioning I/O between operating systems helps to maximize the performance. Further RAM can also be divided but speed of execution limits the partitioning. For the same reason RAM size can be increased to avoid delay.

- **DATA SHARING BETWEEN DIFFERENT OPERATING SYSTEM**

WARP test bed introduces a virtual Ethernet connection between instances of Lab View real time and windows XP running on the same controller. This connection is implemented in system memory and enables seamless porting of applications written for traditional real time systems.

- **BETTER USE OF MULTI CORE HARDWARE**

As number of multi processors are increasing on the same chip abruptly because of VLSI technology, because of which there is a need of parallel processing of these multi processors. Hence timing constraint is the most important feature which is overcome by real time processing.

1.4 Overview of MIMO Hardware Test Beds

Wireless test beds have traditionally been implemented on general –purpose, sequential, Digital Signal Processors (DSP) or on Application specific Integrated Circuits (ASIC).ASIC is fast and power-efficient. But there are some short comings of ASIC. The short comings of DSP's and ASIC's is overcome by FPGA for real time signal processing.

Multiple-antenna systems, also known as multiple input-multiple output (MIMO) radio, improve the capacity and reliability of radio communication systems. Of considerable concern however is the huge complexity involved in the implementation of such systems. Therefore, the design of low complexity, low cost, MIMO systems that keep most of the advantages and benefits of the full-complexity system have gained significant attentions recently. There has recently been strong research activity and interest in the area of test beds for evaluating and developing MIMO wireless systems. Depending on the research

requirements, MIMO test beds can generally be characterised into three types, software-defined, high performance real time based, and FPGA or digital signal processor (DSP) based. The first type are used to simply transmit data that has been generated offline, then process the results off-line as well. Here the focus is on developing software to implement different algorithms of interest to be tested across the air and can be considered as a Software Defined Radio (SDR). A common feature of this type of testbed is the ability to utilise MATLAB or a similar environment to generate the signal to be sent, transmit across the air via the testbed which returns received samples to be processed off-line. Often the test beds are synchronised with a common clock to simplify the frame and sampling timing between test beds. This type of test bed provides a valuable tool for simplifying the use of real channels in research. However, when the intended testbed use includes developing hardware algorithm implementations, then inclusion of high performance FPGA or DSP cores is required to facilitate real-time processing. There are many examples of such systems which often utilise multiple FPGA's and DSP's. For example, the WARP MIMO Testbed supports 2x2 MIMO systems using the 2.45GHz band. This testbed is controlled using MATLAB scripts to send and receive data. Finally, there are test beds that offer modest real-time hardware capabilities, being in the middle of the two groups already discussed. This testbed also had the added requirement of being portable to allow channel measurement experiments to be carried out with relative ease.

1.4.1 Introduction to WARP FPGA XC4VFX100

WARP is Wireless Open Access Research Platform. WARP FPGA board is a real time platform on which real time implementation can be done. The WARP board is equipped with radio nodes which are responsible for the processing of signals to be transmitted and received. The input samples are transmitted through the antenna associated with the transmitting radio node of WARP FPGA board. These samples are then received by the antenna associated with receiving radio node of WARP FPGA board.

WARP Lab is a framework which brings together WARP and MATLAB. With WARP Lab, you can interact with WARP nodes directly from the MATLAB workspace and signals generated in MATLAB can be transmitted in real-time over-the-air using WARP nodes. This facilitates rapid prototyping of physical layer (PHY) algorithms.

1.4.2 System Model

The host PC and WARP node are the two devices between which interaction takes place. The host PC includes the main M-Code and its sub modules such as functions. The user creates in the MATLAB the samples to be transmitted. The MATLAB code can be run

and associated with WARP bard only through Ethernet interface. The samples to be transmitted are downloaded to buffers assigned as transmitters through Ethernet with the help of radio controller and radio bridges. The I/Q signals enters the transmitter buffer through and are sliced into I and Q signals individually. The analog to digital converter is given input in I/Q form whose amplified output is then up converted to increase the frequency. The user sends a trigger to transmitter and receiver nodes. The interpolated RF signal is then amplified and then transmitted through transmitting antenna. Upon reception of this trigger to transmitter and receiver nodes. Upon Reception of this trigger samples are transmitted over air and captured in real time. The user reads the captured samples from the receiver node to MATLAB workspace. Received samples are processed offline in MATLAB. Downloading of the signal from host PC containing MATLAB and its transmission and reception is shown in figure 1.2 below:

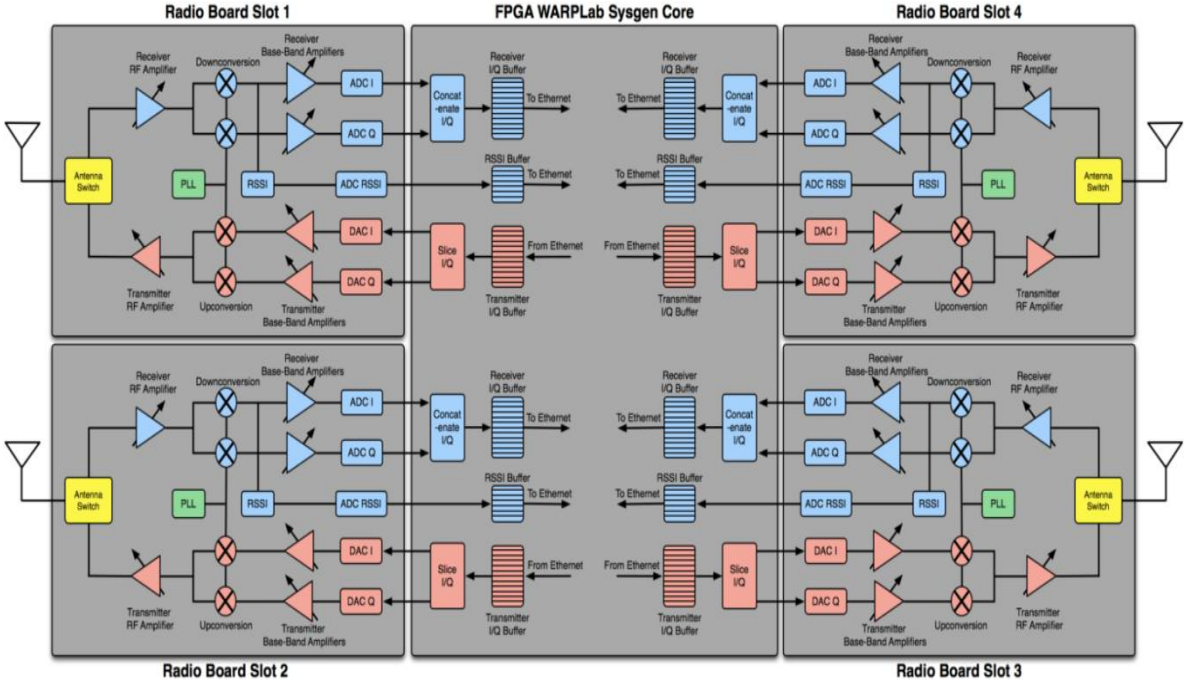

Figure 1.2 Internal Architecture of WARP Board

1.5 Objective of Thesis

- Study and implementation transceiver on WARP FPGA board.
- Implementation of Alamouti scheme for different number of transmitter and receiver antennas for different modulation techniques on WARP test bed.
- Transmission of image using Alamouti STBC for different number of transmitter and receiver antennas through WARP test bed.
- Performance evaluation of Peak Signal to Noise Ratio (PSNR) and Quality Index (Q-index) of grey scale image with different modulation techniques.

- Comparison of results obtained through Software and WARP test bed.

1.6 Outline of Report

In this thesis the Performance of Alamouti STBC for different modulation techniques after implementation on WARP test bed is presented. The remaining of thesis is organised as follow:

In chapter 1 Introduction of Real Time system, its benefit and an overview of MIMO hardware test bed is presented.

In chapter 2 Literature Review for Real Time systems, WARP FPGA board and Alamouti STBC is presented.

In chapter 3 Description of WARP test bed and its various modules used in signal processing, signal transmission and signal reception is presented.

In chapter 4 MIMO communication system and discussion of its various blocks is presented.

In chapter 5 Simulation Parameters and Details are discussed.

In chapter 6 Results obtained through WARP test bed are presented and compared with the simulated results and discussions are presented.

CHAPTER 2
LITERATURE SURVEY

2.1 Introduction

Prior to stating of thesis, it is important to have a deep understanding on the existing pages of hardware test bed, MIMO technology, diversity techniques and image transmission principle. The main sources of information for the thesis are books, journal papers and conference papers. This chapter include overview of the work done in research paper on Real Time implementation.

2.2 Research Paper Literature Review

"J .Sifakis and S.Tripakis" [1] proposed **"Building models of real time systems for application software".** Timed models can be built in real time by adding constraint to the application software. The constraints taken into account for building models are the execution times of the statements, the behaviour of system's external environment and scheduling policies. The analyzable timed model of real time can be build by composing a high level language code.

"M.A.Hannan and A.Hussain" [2] proposed **"Bit error rate for modulation scheme using Software Defined Radio"**. BPSK modulation scheme for SDR can be employed to pick constellation size that best offers the reconstructed signal quality for each average SNR.BPSK has the better quality for a given SNR and due to this reason it is used as basic mode for each physical layer since it has maximum coverage range among all transmission modes.

"Jose A. Garcia-Naya, David Ramirez, Jose M. Torres-Royo et.al" [3] proposed **"Performance of STBC with real data"** for both LOS and NLOS scenarios, the blind channel estimation technique provides similar BER performance than the pilot aided method, with a slight increase in the effective data rate and a moderate increase in the computational complexity of the detector. On the other hand, the differential STBC presents, as expected, a 3-dB penalty in comparison with coherent schemes, but it can be of interest due to its simplicity and its potential advantage in rapidly time-varying channels.

"J Dowle, S. H. Kuo, K. Mehrotra, I. V. McLoughlin" [4] proposed **"An FPGA-Based MIMO and Space-Time Processing Platform".** It is a scheme that is primarily concerned with the challenges of MIMO and ST implementation within a baseband signal. According to **J Dowle et.al** in processing context, the use of programmable FPGA

logic for performing MIMO and space-time baseband signal processing requires less effort, and resulted in a more stable system than a similar DSP-based implementation.

"T. Kaiser, A. Bourdoux, M. Rupp, U. Heute" [5] proposed **"Implementation Aspects and Test beds for MIMO systems".** The analysis of several MIMO implementation challenges for current and for future wireless communication standards. The authors classified the accepted thirteen submissions into four major categories: a) hardware-oriented prototypes, b) flexible test beds, c) analog issues, and d) fast algorithms.

"S. M. Alamouti" [6] proposed **"A simple two-branch transmit diversity scheme".** In this paper author has shown that while using two transmit antennas and one receive antenna the proposed scheme provides the same diversity order as maximal-ratio receiver combining (MRRC) with one transmit antenna, and two receive antennas. An obvious application of the scheme is to provide diversity improvement at all the remote units in a wireless system, using two transmit antennas at the base stations instead of two receive antennas at all the remote terminals. The scheme proposed by author in this paper does not require any feedback from the receiver to the transmitter and its computation complexity is similar to MRRC. When compared with MRRC, if the total radiated power is to remain the same, the transmit diversity scheme has a 3-dB disadvantage because of the simultaneous transmission of two distinct symbols from two antennas. Otherwise, if the total radiated power is doubled, then its performance is identical to MRRC.

"Chris Dick, Patric Murphy, J. Patric Frantz" [7] proposed **"FPGA implementation of a multiple antenna wireless communications system based on Alamouti's transmit diversity scheme".** In this paper the receiver is assumed to have perfect knowledge of every channel between its antennas and those of the transmitter. Such perfect channel knowledge is often assumed in the process of developing wireless algorithms but is rarely available in practice.

"Z.Wang and A.C. Bovik" [8] proposed **"A new universal objective image quality index"** which is easy to calculate and applicable to various image processing applications. Instead of using traditional error summation methods, the proposed index is designed by modelling any image distortion as a combination of three factors: loss of correlation, luminance distortion, and contrast distortion. In this paper the experimental results indicate that it outperforms the MSE significantly under different types of image distortions, the performance of MSE is extremely poor in the sense that images with nearly identical MSE are drastically different in perceived quality. The basic idea

introduced in this paper is a promising starting point for the future development of more successful image and video quality assessment methods.

"Duan Jinghong, Deng Yaling Liang Kun" [9] proposed **"Development of Image processing System Based on DSP and FPGA".** Real-time image processing system that is widely used in many field, it is required to have high speed. In order to satisfy the demand, an image processing system structure based on DSP and FPFA is presented, that is DSP is used as advanced image processing unit and FPGA as logic unit for image sampling and display. The hardware configuration and working principle is introduced firstly, and then some key problems which include of image data stored mode, color space conversion and image transmission based on EDMA are described. Finally the program flowchart for developing image processing software is given. The developed system can acquire image, display image and make some image processing operations which include of geometry transform, orthographic transform, operations based on pixels, image compression and color space conversion. The developed system can meet the real-time requirement and has been used in our teaching.

"V. Roman, K.R. Namuduri" [10] proposed **"A combined source-channel diversity scheme for image transmission through wireless channels with flat fading and noise".** The proposed scheme in this paper combines the multiple descriptor coding (MDC) and space time block coding (STBC) techniques to achieve diversity at both source and channel. In the proposed scheme, the input image is transmitted using multiple transmit and receive antennas (two transmit antennas and one receive antenna). The total diversity provided by the system includes both source and channel diversity making the proposed scheme highly suitable for image and video transmission over wireless channels.

"Xiang Nian Zeng, A. Ghrayeb" [11] proposed **"A comprehensive performance analysis of combined convolutional coding and space-time block coding with receive antenna selection".** In this paper from the experimental results the authors has shown that the advantages of concatenating a STBC code with an outer CC code is the significant increase in the diversity order. But on the other hand, the consequence of this concatenation is a reduction in the bandwidth efficiency, which may become crucial in high data rate applications. One solution to this problem would be to replace the outer CC code with a trellis-coded modulation (TCM) code in order to compensate for the code rate of the outer code.

"U.K. Kumar, B.S. Umashankar" [12] proposed **"Improved hamming code for error detection and correction"**. In the proposed improvement the redundancy bits will be appended at the end of data bits. This eliminates the overhead of interspersing the redundancy bits at the sender end and their removal at the receiver end after checking for single-bit error and consequent correction, if any. Further the effort needed in identifying the values of the redundancy bits is lower in the proposed novel method. Hamming code is normally used for transmission of 7-bit data item. Scaling them for larger data lengths results in a lot of overhead due to interspersing the redundancy bits and their removal later. In contrast, the method proposed by authors in this paper is highly scalable without such overhead. Because of this feature it is suitable for transmission of large size data bit-streams with much lower redundancy bits per data bit ratio. Because of this feature this new method is suitable for transmission of large size data bit-streams as long as there is likelihood of at the most single-bit error during transmission.

"Xuejing Zhang, Lin Xue & Jinping Li" [13] proposed the **"Co-decoding principles of Hamming codes"**. On the basis of this principle, a kind of efficient software error-correcting algorithm is presented**.** This paper discusses the software implementation of hamming code encoding and decoding method and it is the basis for other methods. For such encoding and decoding of the process, we can also use the hardware to realize ,and the overall efficiency will be increased, but the large number of matrix generation, such as transpose and multiply-add operations significantly increases the system overhead and hardware complexity, extended product development cycles, and increase costs. Thus, in some less demanding real-time occasions, such algorithm is more simple and flexible than implemented in hardware.

"S.S. Sarnin, N Kadri, A.M. Mozi et al." [14] Proposed the **"Performance analysis of BPSK and QPSK using error correcting code"**. To calculate the bit error rate, different types of error correcting code were used through an Additive White Gaussian Noise (AWGN) channel. Bose- Chaudhuri-Hocquenghem (BCH), cyclic code and hamming code were used as the encoder/decoder technique. In this paper the performance was determined in term of bit rate error (BER) and signal energy to noise power density ratio (E_b/N_o). Both BPSK and QPSK were also being compared in the symbol error capability known as t in which expected that the performance is graded in response to the increasing of value of t.

"R.B. Ertel & P. Cardieri" [15] provided a review of the key concepts in spatial channel modeling and present emerging approaches. This article has also provided a review of a

number of spatial propagation models. These models can be divided into three groups. a) General statistically based models, b) More site-specific models based on measurement data, c) Entirely site-specific models. The first group of models are useful for general system performance analysis. The models in the second group can be expected to yield greater accuracy but require measurement data as an input .An example from the third group of models is Ray Tracing, which has the potential to be extremely accurate but requires a comprehensive description of the physical propagation environment as well as measurements to validate the models.

"D. B. Smith and T. D. Abhayapala" [16] proposed **"Bit-Error-Rate (BER) for modulation technique using Software defined Radio".** In this paper the idea for the performance analysis of maximal ratio combining (MRC) using BPSK modulation in spatially correlated Rayleigh fading channels with imperfect channel knowledge are represented in terms of antenna array configuration and parameters of scatterer distributions has been described.

"Y. Linn" [17] proposed **"A New Architecture for Coherent M-PSK Receivers".** This architecture has several unique characteristics. (a) It is very suitable for compact implementation within an FPGA (Field Programmable Gate Array), (b) it is resilient to AGC (Automatic Gain Control) imperfections, (c) It is particularly optimized for implementation using fixed-point binary arithmetic. Also channel signal-to-noise ratio (SNR) estimator for M-ary phase shift keying (M-PSK) and differential M-PSK is proposed which does not require prior carrier synchronization, has a compact Fixed-point hardware implementation suitable for Field-programmable gate arrays.

"Mostafa Wasiuddin Numan, Mohammad Tariqul Islam and Norbahiah Misran" [18] proposed **"Implementation of Alamouti Encoder Using FPGA for MIMO Testbed"**. The design and implementation of a Space Time Block Coding (STBC) encoder is based on Alamouti scheme on a Xilinx® Virtex™-4 XC4VLX60 Field Programmable Gate Arrays (FPGA) devices. This encoder is a part of MIMO testbed, equipped with multiple element antennas (MEA) at both ends of the link. The task of this Alamouti encoder is to appropriately encode the modulated symbols to achieve both time and spatial diversity. The encoder for the MIMO testbed is developed based on modular design which simplifies system design, reduces development time, eases hardware update and facilitates testing the various modules in an independent manner.

"M.T.Islam, M.W.Numan, N.Misran"[19] proposed **"Design and implementation of Alamouti Encoder for 4G wireless System"**. Multiple-input multiple-output (MIMO)

systems are called to play a crucial role in fourth Generation (4G) wireless systems to provide advanced data services. This paper addresses the design and implementation of a MIMO encoder that is based on Alamouti scheme on a Xilinx® Virtex™-4 XC4VLX60 Field Programmable Gate Arrays (FPGA) devices. This encoder is a part of MIMO testbed, equipped with multiple antennas at both ends of the link which appropriately encodes the modulated symbols to achieve both time and spatial diversity. The encoder for the MIMO testbed is developed based on modular design which simplifies system design, eases hardware update and facilitates testing the various modules in an independent manner**.** 4G wireless systems employ multiple antenna techniques to provide high performance while maximizing spectral efficiency. This prevalence of MIMO systems highlights the need for designed platforms to evaluate such algorithms under realistic conditions.

"Simon Haene,David Perels and Andreas Burg" [20] proposed **"A Real-Time MIMO Transceiver System Design, FPGA Implementation, and Characterization".** MULTIPLE-INPUT multiple-output (MIMO) technology combined with channel coding, has recently attracted significant attention. MIMO offers high spectral efficiency through spatial multiplexing. Due to this significant advantage, the combination of these two technologies constitutes the basis for many next generation wireless communication systems.

"H.K. Mecklai and R.S Blum" [21] proposed **"Transmit Antenna Diversity for Wireless Communications"**. In this paper both transmit and receive diversity are being explored to increase the capacity and improve the performance of wireless communication systems. Transmit diversity is the focus of this paper. Multiple antennas transmit amplitude and phase weighted signals to a single antenna for each user. Fading coefficients were assumed to vary at a slow enough rates *so* that reliable estimates can be obtained at the transmitter. Transmitter weights are derived to maximize the Signal to Interference Noise Ratio (SINR) at the output of the matched filter based receiver for each user.

"Adrian Tarniceriu, Bogdan lordache, Silvian Spiridon" [22] proposed **"An Analysis on Digital Modulation Techniques for Software Defined Radio Applications"**. In this paper the analysis of typical digital modulation techniques used in today's wireless communications has been done. The paper presents the characteristics of the modulation techniques and determines the figure of merit for each particular modulation: Bit Error Rate (BER) vs. Signal-to- Noise Ration (SNR). The analysis emphasizes the importance

of such figure of merit in the context of Software Defined Radios (SDR). This paper presented an analysis of the modern modulation techniques.

"Feng Ge and Charles W. Bostian" [23] proposed **"SDR Implementation Issues: Rf Front End Nonlinearity and Dynamic Computing Resource Allocation"**. In this paper author addresses two practical issues governing Software Defined Radio (SDR) performance that are often overlooked: RF front end nonlinearity and dynamic computing resource allocation. Current SDR performance still depends heavily on analog radio frequency (RF) technologies. Inter-modulation and other nonlinear effects in these devices make it very challenging to create an RF front-end that is applicable to a variety of signals with widely differing centre frequencies, modulation bandwidths, and power levels. Unanticipated inter-modulation products can seriously degrade receiver performance. Digital signal processing in wireless communication is fundamentally a real-time task. Achieving real-time performance in SDRs puts stringent requirements on dynamic computing resource allocation; these requirements may be much higher than those in conventional digital radios.

"Chris H. Dick, San Jose" [24] proposed **"Design and Implementation of High-Performance FPGA Signal Processing Datapaths for Software Defined Radios".** In this paper authors has described how many of the functions required in a hardware test bed can be realized in an FPGA. The FPGA resources of particular interest to the signal processing engineer are configurable dual-port block memories, distributed memory and the multiplier array. FPGA based signal processors are being employed in a diverse range of signal processing applications for reasons of performance, economics, flexibility and power consumption. FPGAs offer great flexibility, which can, for instance, enable designers to service multiple standards. DSP microprocessors, even with advanced architectural extensions (very long instruction word (VLIW), super-scalar, etc.) do not satisfy the arithmetic or I/O requirements of a modern communication signal processing engine. Advanced field programmable gate array technology offers a solution.

"S. Weiss, A. Shligersky, S. Abendroth, et. al." [25] "Proposed Software Defined Radio Testbed Implementation". In this paper, the digital-to-analog and analog-to-digital conversion are performed close to the radio frequency so as to implement modulation, demodulation, channel coding and other required processing tasks in software. SDR test-bed comprises a transmitter and receiver, which is implemented on FPGA performing the baseband operations. The aim of our testbed is to provide a wireless link between two PCs, which are connected to the baseband FPGA via Ethernet

Connections. We aim to achieve re-configurability of the testbed by using adaptive modulation with modulation levels dependent on channel SNR.

"S. Glass, V. Muthukkumarasamy, M. Portmann" [26] proposed **"A Software-Defined Radio Receiver for APCO Project 25 Signals"**. In this paper author analyze traffic from public safety communications and uses APCO Project 25 (P25) standard. P25 is the digital communications standard. It is used as emergency first-responder). It provides low level access to the actual message traffic using the Wire Shark packet sniffer. A P25 radio system consists of both fixed and mobile equipment. P25 systems encode all voice traffic using the IMBE vocoder. Using an SDR approach enables a single station to simultaneously process many analog and digital signals because processing is partitioned into blocks with 20 well-defined interfaces. The demodulation stage can be easily replaced to allow for reception of different modulation schemes whilst sharing the common code for packet assembly and decoding. Higher bandwidth requirements are met by Cognitive radio by opportunistic use of bands that are underutilized by their primary users. SDR approaches can ensure interoperability and backward-compatibility with existing equipment. Daughter boards provide for frequency translation, amplification and filtering to enable receive and transmit access to the VHF and UHF bands used for public safety communications. If a radio needs a signal-processing block that isn't present then it can be written (often using an existing block as a starting point) and added to the framework. The Receiver produces digital audio as its output and sends the decoded P25 frames to the WireShark network protocol analyzer where they can be analyzed in detail. The WireShark network protocol analyzer is used to recognize, filter and dissect P25 network traffic.

"Junruo Zhang, Y.V. Zakharov, R.N. Khal" **[27]** proposed **"Optimal detection scheme for STBC MIMO systems in spatially correlated Rayleigh fast fading channels with imperfect channel estimation"**. In this paper author has compared the performance of proposed scheme with that of traditional mismatched detectors treating channel estimates as perfect in spatially and temporally correlated fading channels. The channel time variations are approximated by using the basis expansion model (BEM). Specifically, the discrete prolate spheroidal basis functions are used. In both spatially uncorrelated and spatially highly correlated MIMO Rayleigh fast fading channels, the optimal detector significantly outperforms the mismatched detectors including the one exploiting minimum mean square error channel estimates. The optimal detector does not estimate the channel explicitly but jointly processes the received data and pilot symbols to

recover the data. We have investigated the optimal detector and compared its performance with that of traditional mismatched detectors with ML, regularized ML or MMSE channel estimates in MIMO fast fading channels. The optimal detection significantly outperforms the mismatched detection for space-time block coded signals in both spatially uncorrelated and spatially highly correlated MIMO Rayleigh fast fading channels.

"Lihua Yang, Bingke Yang, Guangliang Ren, Zhiliang Qiu" [28] proposed **"Improved STBC transmit diversity scheme in high speed mobile environment".** The effect of the fast time varying channel on Almouti space-time block coding (STBC) scheme is analyzed in high speed mobile environment, and an improved scheme is proposed. Simulation results show that performance of the proposed method is much better than that of the Almouti STBC scheme when the vehicle speed is greater than 350 km/h. To effectively combat the fast fading in the high speed mobile environment .Author proposed an improve STBC scheme for OFDMA systems. The interference of the fast time varying channel on the STBC scheme is greatly reduced. The proposed method can also be used in the transmit diversity systems with two transmit antennas and two receiving antennas. Moreover, the ideal of the proposed scheme can also be applied to the space-frequency block coding (SFBC) scheme in the wireless channel with strong frequency selective fading.

"Vahid Tarokh, Hamid Jafarkhani, and A. Robert Calderbank" [29] proposed **"Space–Time Block Coding for Wireless Communications: Performance Results"**. The performance of space–time block codes which provide a new paradigm for transmission over Rayleigh fading channels using multiple transmit antennas is documented. Data is encoded using a space–time block code, and the encoded data is split into n streams which are simultaneously transmitted using n transmit antennas. The received signal at each receive antenna is a linear superposition of the n transmitted signals perturbed by noise. Maximum likelihood decoding is achieved in a simple way through decoupling of the signals transmitted from different antennas rather than joint detection. This uses the orthogonal structure of the space–time block code and gives a maximum likelihood decoding algorithm which is based only on linear processing at the receiver. Author review the encoding and decoding algorithms for various codes and provide simulation results demonstrating their performance. In this paper it is shown that using multiple transmit antennas and space–time block coding provides remarkable performance at the expense of almost no extra processing.

"M.P.Fitz, J.Grimm, J.V.Krogmeier" [30] proposed **"Code design for transmitter diversity in fading". This paper presents code design principles and gives some example** codes for high performance transmitter diversity systems in frequency non selective Rayleigh fading.

"R.Ayoubi, J.P. Dubois, O. Abdul-Latif" [31] proposed **"FPGA Implementation of a Novel Receiver Diversity Combining Technique for Wireless SIMO Systems"**. In this paper, we study FPGA implementation of a novel receiver diversity combining technique, RMSGC for Wireless transmission over fading channels in SIMO systems. The main drawback of algorithms that require massive parallelism RMSGC is that it is a non-linear technique, thus parallelism of the logic resources as well as successful FPGA implementation of it using pipeline techniques is needed as a wireless communication test- large RAM blocks, DSP slices etc) On the FPGA testbed for practical real-life situations.

"H. Dreizen" [32] proposed **"Content driven progressive transmission of grey scale images"**. In this paper lossless progressive transmission method for grey-scale images which concentrates early transmission efforts on areas of greater image information content is described. The receiver does not have a priory knowledge of which image areas are to receive preferential treatment, and the preferential level of resolution is the pixel. The method proposed in this paper makes use of simultaneous geometric and information content decompositions. The proposed method is computationally simple with a complexity which grows linearly with the number of pixels. Compression achieved approaches that obtained by non progressive lossless methods, and is approximately the same as for homogeneous progressive lossless methods. Extensions of the method for progressive transmission with limited distortion and greater compression are also discussed. By selection of a mutually beneficial image information measure and image coding technique, the image is simultaneously decomposed by geometry and entropy. The individual node selection bits serve to define the non homogeneous geometric decomposition decisions. The collection of node selection bits and their relationship to the quad-tree traversal serve to partition the transmission into passes corresponding to decreasing levels of sub image entropy. With this dual utilization of node selectors, the order of transmission can be controlled by image content with minimal overhead.

"A. Hore, D. Ziou" [33] proposed **"Image Quality Metrics: PSNR vs. SSIM"**. In this paper, author has analysed two well-known objective image quality metrics, the peak-signal-to-noise ratio (PSNR) as well as the structural similarity index measure (SSIM). A

series of tests realized on images extracted from the Kodak database gives a better understanding of the similarity and difference between the SSIM and the PSNR. In this paper, we have undertaken a theoretical study to compare the PSNR and the SSIM quality metrics by analysing their analytical formula. The study has revealed that a simple analytical link exists between the PSNR and the SSIM. We have also undertaken an experimental study in order to assess the sensitivity of the PSNR and the SSIM to these degradations, that is how the values of the Parameter associated to each of these degradations affect the values of the PSNR and the SSIM. The study has revealed that the PSNR is more sensitive to additive Gaussian noise than the SSIM. As a final conclusion, it appears that the values of the PSNR can be predicted from the SSIM and vice-versa. The PSNR and the SSIM mainly differ on their degree of Sensitivity to image degradations.

"Tolga M. Duman and Ali Ghrayeb" [34] proposed **"Coding for MIMO communication system".** MIMO wireless systems have received a great deal of attention recently, in part due to the promise of increased throughput, extended range, and improved reliability. Achieving the gains of the MIMO channel requires coding that can take advantage of these channel resources. This work studies the performance of different concatenated space-time coding and outer channel coding and develops some practical guidelines for coding design of MIMO wireless systems.

"Martin and Christ" [35] proposed **"MIMO Channel Characterization and Joint Channel Estimation and Detection in Digital Communications".** The use of antenna arrays in wireless digital communication systems provides many advantages. The spatial freedom of the array offers the possibility to increase range, combat fading and reject interference. By employing multiple antennas at transmitter and receiver sites, multi-input Multi-output (MIMO) architectures are formed. The capacity, the achievable error-free data rate, of such systems is known to be several times that of their single antenna counterparts. While multi-channel configurations have received considerable attention during the last couple of years there are still several open issues. This thesis consists of two parts. In the first a statistical characterization of some fundamental properties of MIMO channels are presented. The second introduces some tools for analysing joint estimation and detection algorithms in multi-channel receivers. Closed form approximations of the channel matrix squared singular values and the MIMO channel capacity in the presence of correlated fading are considered. Limiting distributions of these properties are derived as the number of antennas on either side of the system is

increased. Spatial correlation is allowed according to a realistic channel model and the derived distributions have the advantage of being closed form. Simulations and channel measurements indicate that the asymptotic distributions

Provide a good approximation of the true distributions also for realistic antenna array sizes.In order to investigate the performance of joint estimation and detection in multi-channel receivers, a Cramer Rao bound and an iterative algorithm are proposed. The proposed methods allow for burst non synchronized interference and a generalized scheme of adding training redundancy to a data frame. Simulations and computations of the derived bound are presented that indicate that using elaborate training schemes can improve error rate performance and robustness to non-synchronized.

"S. Caban, C. Mehlfuhrer, L.W. Mayer, M. Rupp" [36] proposed **"2x2 MIMO at Variable Antenna Distances".** Various publications have drawn a precise picture on how correlation and capacity change when decreasing the receive-antenna distance of a 2×2 MIMO transmission to less than 0.1 λ; however, little is known on how today's commonly employed coding schemes actually perform under such harsh conditions. In this paper, author has evaluated—by measurements with a testbed—the uncoded BER over antenna distance performance of: spatial multiplexing, a linear dispersion code, the Golden Code, as well as Alamouti coding. We show, that even at very small antenna distances, a significant gain compared to an ordinary 1×2 SIMO transmission can be measured.

"J.W. Wallace" [37] Proposed **"A real-time multiple antenna element testbed for; MIMO algorithm development and assessment".** Authors have presented a real-time DSP-based testbed capable of implementing fairly advanced space-time MIMO architectures. Utility of the system was demonstrated by describing a real-time video application and showing SER performance **of** a simple space-time decoding scheme. In the future, we intend to write software for more advanced space-time algorithms to fully utilize the resources of the platform. Such effort will demonstrate real-world performance Of existing algorithms and will allow a feasibility assessment of these proposed algorithms.

"Zhu Xiangbin" **[39]** proposed **"Support QOS in Open Real Time Systems"** With the development of computer systems, the real time systems with different kinds of real-time applications and non-real-time applications are becoming more and more popular. At the same time, more and more multimedia applications make real-time system to support QoS. Based on the real-time Systems, the paper proposes a model of Linux based open

real-time systems with QoS support. Firstly, the paper analyzes real-time systems and QoS. Secondly, a windows-constrained CBS is proposed. Then it proposes the scheduling framework of Linux-based open real-time systems.

2.3 Conclusion

The work discussed in literature review is already done by simulations on software. In this thesis the whole work is implemented in real time using WARP hardware test bed.

CHAPTER 3
WARP FPGA DESCRIPTION

Wireless open Access Research Platform (WARP) was developed at RICE University, USA by Murphy brothers. It is a hardware test bed involving FPGA as a main module and developed to be used in the design and testing of wireless MIMO communications systems. WARP board consists of other modules also like analog board, clock board, radio board and their description is given in following sections. The most important module is Radio board which is responsible for the transmission and reception of signal. It is connected to a PC via USB 2.0 or ethernet and uses an on-board FPGA to allow implementation of algorithms in logic, together with provision for multiple radio modules.

3.1 WARP Lab Framework Overview

WARP Lab is a framework which brings together WARP and MATLAB. With WARP Lab, you can interact with WARP nodes directly from the MATLAB workspace and signals generated in MATLAB can be transmitted in real-time over-the-air using WARP nodes. This facilitates rapid prototyping of physical layer (PHY) algorithms.

3.2 WARP MIMO Test Bed Block Diagram

The custom built MIMO Communication testbed is based on a main baseband board capable of controlling up to 4 RF boards. Combining two of these complete systems provides capability for any MIMO antenna configuration scenario up to 4x4. The digital board provides an interface to a host PC via USB or Ethernet connection, and an FPGA to process baseband signals to ADC's and from DACs on the radio modules. The baseband design is centered on an Altera Stratix Xilinx virtex-4 XC4VFX100FFG1517-11. The block diagram and pictorial view of WARP test bed is shown in Figures 3 and figure 4.

A challenge in traditional MIMO testbed design is the amount of data that must be transferred between the baseband and radios. For example, using 4 receivers with 14-bit ADC's at 40MHz sampling rates requires a transfer rate of 4.48Gbps. By using FPGA at the core of the design, the testbed is able leverage the high I/O capability on PLD's and achieve the high data transfer rates. To allow the capture of long frame lengths, additional storage is provided to the FPGA using an external static random access memory (SRAM). This memory can store 144Mbits of I/Q data, which is equivalent to a transmission block length of 15.7ms using 12 bit I/Q data. This frame length is adequate for testing short burst transmissions.

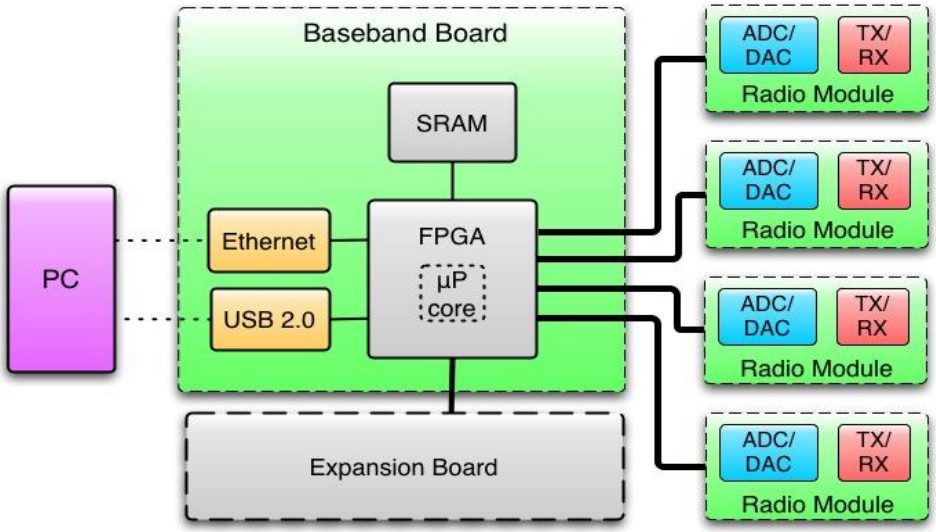

Figure 3.1 Block diagram of WARP test Board

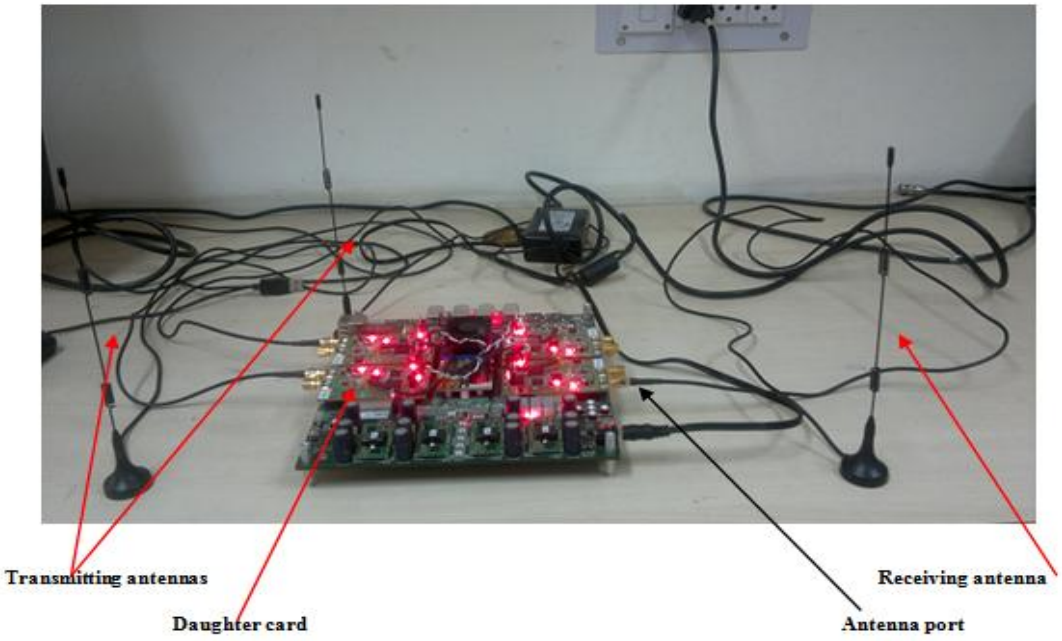

Figure 3.2 Pictorial view of WARP test bed

3.2.1 Radio Modules

The radio frequency (RF) modules developed use the 2.4GHz to 2.5GHz ISM band, and provide a transmission bandwidth up to 40MHz via the Maxim MAX2829 transceiver chip. The I/Q interfaces of the MAX2829 are connected directly to the Radio Board's ADC and DAC. The transceiver's control interfaces are connected to the daughter card headers, enabling direct control from the FPGA. These implement a direct conversion process, removing the need for IF stage design. Moreover, the MAX2829 chips are designed for use in MIMO applications, with a mode to enable clock synchronisation

between multiple transceiver chips. The block diagram and internal architecture of one of the four RF modules is shown in figures below:

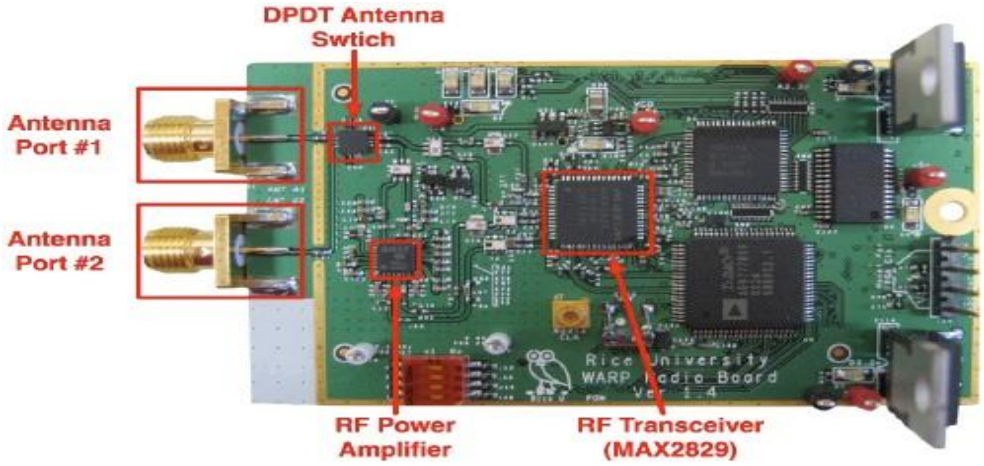

Figure 3.3 WARP FPGA RF module

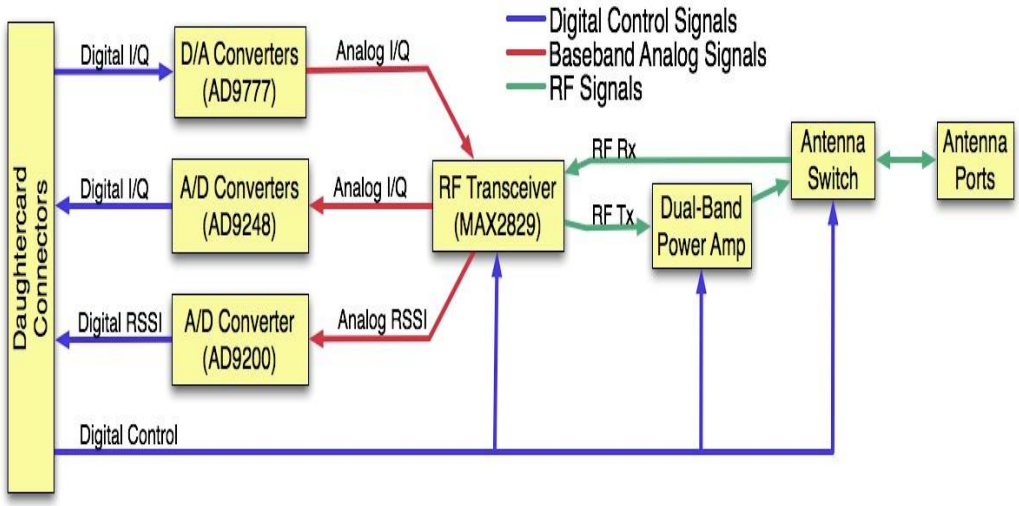

Figure 3.4 Internal architecture of one RF module

Additionally, a power amplifier and T/R switch are incorporated. Each RF board contains I/Q ADC and DAC's capable of 14 bit operation and connect directly to the baseband board FPGA. The ADC can be operated at up to 80Msps whilst the DACs are rated at 500MHz, allowing more flexibility for pulse shaping. All RF boards use a common 40MHz clock generated on the baseband board that can be adjusted using firmware to provide frequency offset corrections. The ADC/DAC can run off the same clock as the transceivers, or a user defined clock by configuring the FPGA PLLs. An external clock source may also be used via a SMA connector if desired. Most configurable options for the RF module components are carried out through serial interfaces, with some direct I/O connections from the FPGA , Antenna Ports **.**The radio board has two antenna ports. Both are fitted with SMA jacks (standard polarity female connectors). The two ports are

connected to a DPDT RF switch. The other side of the switch is connected to the transmit and receive paths leading back to the RF transceiver. The antenna switch is controlled by a 2-bit digital signal, driven by the FPGA. In the default configuration, Port 1 is used for both transmit and receive and Port 2 is unused. This configuration requires the antenna switch's state be changed every time the radio changes between receive and transmit modes. This behaviour is implemented in the radio controller driver and hardware.

3.2.2 WARP Clock Board

Figure 3.5 WARP Radio Clock Board

There are three clock domains on the Radio Board, as described below.

a) RF Reference Clock

The MAX2829 transceiver requires a reference clock which is multiplied up by its PLL to form the RF carrier. This must be a 20MHz or 40MHz clock and must be driven into the Radio Board's MMCX jack. In standard WARP kits, the WARP Clock Board drives this signal at 20MHz. If multiple Radio Boards are driven by the same RF reference clock, their RF carriers will be synchronous, though there will be a phase offset resulting from their PLLs locking at different times.

b) I/Q Sampling Clock

The I/Q ADCs and DACs are driven by a common clock. This clock is produced on an on-board clock buffer (an Analog Devices AD9513). The source clock for this buffer comes from an off-board source driven into a 4-pin connector. In standard WARP kits, the WARP Clock Board drives this signal at 40MHz. If multiple Radio Boards are used on a single kit, they should all be driven by synchronous and in-phase sampling clocks.

c) **RSSI Sampling Clock**

The dedicated RSSI ADC is clocked from the FPGA via the daughter card headers. Any frequency up to 20MHz is valid. There is no requirement for this clock to be synchronous with other clocks on the Radio Board**.**

3.2.3 External Interfacing

A common support bus provides host interface connections via USB 2 or Ethernet as well as Flash memory and program memory for the Nios II processor core running on the FPGA. The FPGA is the main processing component, under the control of a Nios II core. This core runs custom software that provides access to and from the host PC to control the testbed. The core interprets host commands and configures the radio modules via control registers. Once the testbed is configured, the host can then begin a test by starting the signal processing block on the FPGA. In the simplest configuration, this block will simply send I/Q data from the host to the transmitters and capture received signals for offline processing by the host. In more complicated scenarios the user can implement algorithms to process baseband signals in a real time environment on the FPGA.

3.2.4 Extending

Additional computational power can be added via a high speed 32-bit bus. The testbed has been designed to enable the direct connection of a Texas Instruments DSP development kit via the Universal Host-Port Interface (UHPI). This bus can also be used to interface to custom ASICs to provide a versatile testing environment. Multiple baseband boards may also be combined to generate MIMO test systems with higher than 4x4 capabilities through common clocking schemes and a small number of control signals.

3.3 WARP Testbed Features

Testbed hardware provides a simple method for testing algorithms over the air. Some key features on the testbed are:

- All baseband processing is on "Baseband Board".
- Interchangeable "Radio Modules" allow different RF bands to be used.
- Up to 4x4 MIMO supported using 2 boards.
- Supports online or offline processing:
- Write VHDL code for online processing in FPGA
- Use PC via USB/ethernet to perform processing offline with MATLAB, C, etc.
- Test beds operating from a single PC have been incorporated into a MATLAB model of 3G LTE system

CHAPTER 4

ARCHITECTURE OF MIMO WIRELESS COMMUNICATION SYSTEM

4.1 Introduction

Wireless communications systems are able to achieve higher throughput than before, with each stage in their evolution. These systems are getting closer and closer to the theoretical maximum throughput specified by Shannon's Equation, which is a function of channel bandwidth and signal-to-noise ratio (SNR). In fact, Shannon's equation for channel capacity reflects the relationship between bandwidth and SNR and is shown below [35]:

$$\text{Channel capacity} = \text{Bandwidth}\,[\log_2(1 + \text{SNR}) \quad (1)$$

According to above equation, the capacity increases linearly with respect to an increase in bandwidth, and is logarithmically related to changes in SNR. The second factor of Shannon's equation that limits system throughput is the channel bandwidth. The bandwidth of a channel is a linear function of its symbol rate. Thus, increasing the symbol rate of the channel increases throughput at the expense of requiring more bandwidth [35]:

$$\text{Bandwidth} = \text{symbol Rate X}\,(1 + f_a) \quad (2)$$

Where f_a is the pulse frequency (in pulse per second).Increasing the symbol rate of a communications channel does not improve its efficiency. Instead, it simply increases the occupied bandwidth. Because the available frequency spectrum is finite, channel bandwidth is typically limited, as illustrated by Figure 4.1.

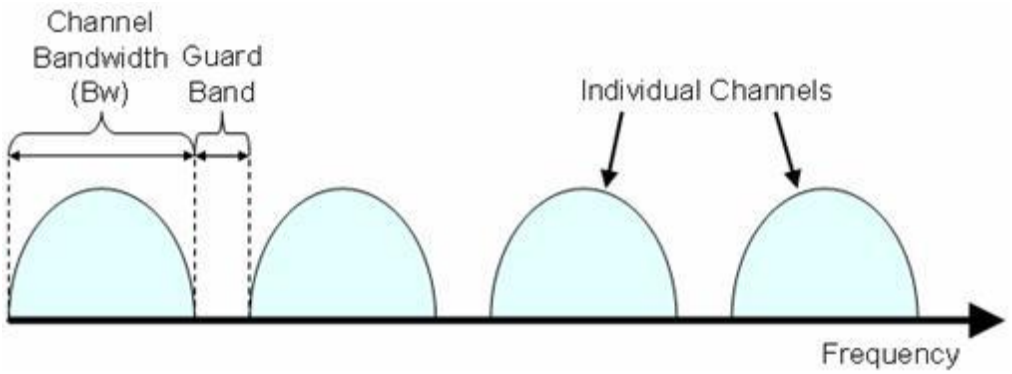

Figure 4.1 Allocation of Frequency spectrum

The width of a channel determines the number of channels that can fit into a given spectrum (wider channels mean fewer channels can fit). Thus, higher symbol rates do not provide a communications system with any gain in efficiency. Moreover, while

Shannon's equation for channel capacity offers a rough idea of the theoretical limits of a communications system, this model assumes that a given channel makes optimal use of the frequency spectrum.

We have witnessed over the past decade or so an unprecedented growth in the demand for providing reliable high-speed wireless communication links in order to support a wide range of applications, including voice, video, e-mail, web browsing, to name a few. Providing such reliable links is challenging due to the fact that, in a wireless environment, unlike many other channels, transmitted signals are received through multiple paths which usually add destructively resulting in serious performance degradations. This phenomenon is normally referred to as *fading*. Furthermore, the medium is normally shared by many different users/applications, thus there is the possibility of significant interference as well. Other challenges for high-speed wireless applications include the scarcity of available bandwidth, highly constrained transmit powers, as well as hardware complexity and cost requirements [34].

With the limited frequency spectrum and the steady increase in the number of new wireless applications or expansion of existing ones, there is a clear problem in being able to accommodate all of them. A simple approach that naturally comes to mind is to use higher order modulation schemes in an effort to improve the bandwidth efficiency. However, one drawback of the naive application of this proposed solution is the poor reliability associated with it. That is, for the same level of transmit power, higher order modulation schemes yield performance that is inferior to that of the lower order modulation schemes. In fact, even for small signal constellations, i.e., low-order modulation schemes (e.g. binary), the reliability of uncoded communications over wireless links is very poor in general [34]. The single most effective technique to accomplish reliable communication over a wireless channel is *diversity* which attempts to provide the receiver with independently faded copies of the transmitted signal with the hope that at least one of these replicas will be received correctly. Diversity may be realized in different ways, including frequency diversity, time diversity, antenna diversity, modulation diversity, etc. We encounter the use of diversity in practical wireless communication scenarios all the time. Channel coding may also be used to provide (a form of time) diversity for immunization against the impairments of the wireless channel. Examples of practical channel codes include convolutional and block codes, trellis-coded modulation, multi-level coding, bit interleaved coded modulation, as well as the recently discovered capacity-approaching coding schemes such as turbo and low-density parity

check codes, and coded modulation techniques. In the context of wireless communications, channel coding schemes are usually combined with interleaving to achieve time diversity in an efficient manner.

As another method, transmit and/or receive antenna diversity, also referred to as *spatial* diversity, represents a powerful means of combating the deleterious effects of fading. Systems with multiple antennas are also referred to as multiple-input multiple-output (MIMO) systems. One of the major advantages of MIMO systems is the substantial increase in the channel capacity, which immediately translates to higher data throughputs. Another advantage of MIMO systems is the significant improvement in data transmission reliability, i.e. very low bit error rates. These advantages are achievable without any expansion in the required bandwidth or increase in the transmit power [34].

In this chapter, various diversity and diversity combining techniques are discussed in detail. The various types of diversity are used to provide the inputs to the diversity combiner. Now, since there are a variety of ways in which the independently fading signal branches can be combined, hence, the three most prevalent space diversity-combining techniques used are the Maximal Ratio Combining, Equal Gain Combining, and Selection Combining. These combining techniques are discussed and analyzed in detail in this chapter. Next generation wireless systems are being designed to provide ubiquitous broadband link access to information infrastructure. Diversity techniques play a vital role in supporting such high-speed connections over radio channels by mitigating the detrimental effects of multi- user interference and multipath fading. It was incorporated verify improved performance in both the statistical and spatial channel models. Diversity is known to reduce channel fading and increase the reliability of the transmitted signal. It is assumed that the signals received at the receiver are uncorrelated. Several diversity schemes were available to choose from including space, polarization, angle, frequency, and time. The independent channels in a fading channel environment are often referred to as diversity branches. Having multiple branches available at the receiver decreases the probability that the signals on each branch will all be in a deep fade.

4.2 Types of Diversity

In this section, we examine the type of diversity that can be used to provide the inputs to the diversity combiner. Most diversity systems are implemented in the receiver instead of the transmitter since no extra transmitter power is needed to implement the receiver diversity system. Since the path between the mobile and base is assumed to be reciprocal,

diversity systems implemented in a mobile will work similarly to those in a base station. There are two general types of diversity schemes.

4.2.1 Macroscopic diversity scheme

The Macroscopic diversity scheme is used for combining two or more long-term lognormal signals, which are obtained via independently fading paths received from two or more different antennas at different base-station sites. The local mean strength varies because of variations of terrain between the mobile transmitter and the base station receiver. If only one antenna site is used, the travelling mobile unit may not be able to transmit a signal to the base station at certain geographical locations because of terrain variations such as hills or mountains. Therefore, two separated antenna sites can be used to receive two signals and to combine them to reduce long-term fading. The selective combining technique is recommended in the macroscopic diversity scheme since other methods require coherent combining that is difficult to achieve when the receivers are some distance apart.

4.2.2 Microscopic diversity scheme

The Microscopic diversity scheme is used for combining two or more short-term Rayleigh signals, which are obtained via independently fading paths received from two or more different antennas but only at one receiving co site. Once the diversity branches are created, any of the combining methods can be used. In mobile wireless communications, multipath fading can cause constructive and destructive interference. A popular method to mitigate the effects of multipath fading is diversity, a process of obtaining multiple independent signal branches through many dimensions including time, frequency, polarization, angle, and space

4.2.3 Space Diversity

Space Diversity, also known as antenna diversity, is one of the most popular forms of diversity used in wireless systems. Conventional wireless systems consist of an elevated base station antenna and a mobile antenna close to the ground. The existence of a direct path between the transmitter and the receiver is not guaranteed and the possibility of a number of scatterers in the vicinity of the mobile suggests a Rayleigh fading signal. Two antennas separated physically by a short distance d can provide two signals with low correlation between their fades. The separation d in general varies with antenna height h and with frequency. The higher the frequency, the closer the two antennas can be to each other. Typically a separation of a few wavelengths is enough to obtain uncorrelated signals.

4.2.4 Receiver Diversity

The collection of independently fading signal branches can then be combined in a variety of ways to improve the received SNR. Since the chance of having two deep fades from two uncorrelated signals at any instant is rare, combining them can reduce the effect of the fades. The three most prevalent space diversity-combining techniques are SC, EGC, and MRC. MRC co-phases the signal branches, weights them according to their respective SNRs, and then takes their sum. MRC is the most complex combining technique, but also yields the highest SNR. The analysis of all of these diversity techniques is presented here.

4.2.5 Transmitter Diversity

In transmit diversity there are multiple transmit antennas with the transmit power divided among these antennas. Transmit diversity is desirable in systems such as cellular systems where more space, power, and processing capability is available on the transmit side versus the receive side. Transmit diversity design depends on whether or not the complex channel gain is known at the transmitter or not. When this gain is known, the system is very similar to receiver diversity. However, without this channel knowledge, transmit diversity gain requires a combination of space and time diversity via a novel technique called the Alamouti scheme [42].

4.3 MIMO System Overview and Need of MIMO System

The equation (1) assumes a communications channel with one transmitter antenna and one receiver antenna (i.e. SISO). Thus, Shannon's equation can be expanded to account for MIMO systems. In MIMO systems, using multiple antennae can increase the effective SNR of the system. Moreover, the mathematical representation of the throughput of a perfectly ideal communications channel can be shown with the following equation [35]:

$$\text{Channel capacity} = \text{Antennae} * \text{Bandwidth} * \log_2(1 + \text{SNR}) \quad (3)$$

Equation (3) illustrates, the channel throughput of MIMO systems can be greatly enhanced by increasing the number of transmit or receive antennae. Thus, MIMO systems are a significant innovation of wireless communications because they enable an increase in throughput of a communications channel without increasing the occupied bandwidth or order of modulation scheme. For this reason, evolving Wi-Fi standards such as IEEE 802.11n utilize the MIMO approach with OFDM to achieve significant channel throughputs. In fact, the specification aims to achieve data throughputs of more than 600 Mb/s for a 40 MHz bandwidth. This is a significant improvement over the 54 Mb/s throughputs in a 20 MHz channel for IEEE 802.11g.

The basic premise of MIMO antennae systems is that the effective SNR of the system can be increased by transmitting unique bit streams with multiple transmit antennae in the same physical channel. This is referred to as spatial multiplexing. By multiplexing the message bit stream across several channels, engineers can increase system throughput linearly according to the number of transmitters used. Note that OFDM uses a similar approach in that it also multiplexes a bit stream across each of its subcarriers. However, in OFDM systems, the symbol rate of each of the subcarriers is proportional according to the number of subcarriers in a given channel. With MIMO systems, the bit stream is multiplexed to multiple transmitters.

4.3.1 Advantages of MIMO system

- It enables the increase of data rates by transmission of several independent multiplexed data streams on the different transmit antennas.
- It can enable robust communications, especially in challenging environments for radio propagation, by sending instead redundant information over the multiple antennas. Multiple data streams enable higher data speeds, while with redundancy under less radio-friendly conditions, if one signal is disrupted by interference, the receiver can recover all data from the other, a benefit known as "diversity".

4.4 Spatial Multiplexing

Spatial multiplexing is the process by which a single data stream is multiplexed into individual data streams. This is a significant departure from the traditional approach of using more of the limited bandwidth resources to increase the data rate. A block diagram of spatial multiplexing is shown in Figure 4.2.

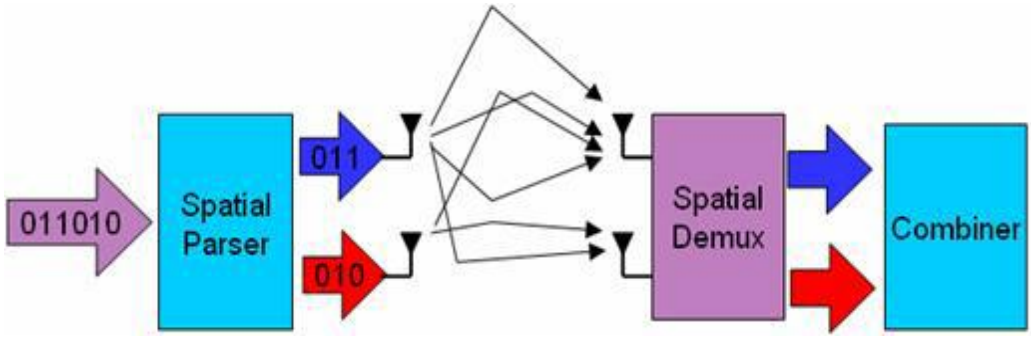

Figure 4.2 MIMO System uses Spatial Multiplexing to Increase Data Rate

As Figure 4.2 illustrates, spatial multiplexing requires multiple transmit and receive antennae. These antennae transmit and receive distinct data streams into the same physical channel. As a result, engineers cannot evaluate the physical channel of a MIMO system in the same way that they can understand other communications channels.

Traditionally, communications channels have been represented by a vector approach such that the signal is known to have an instantaneous amplitude, frequency, and phase. However, a system with multiple transmitters using the portion of the spectrum is interpreted as mere noise if the traditional vector representation of the physical channel is used. One way to view the physical channel is with a series of equations by which the received signal can be related as a function of the channel characteristics. For a single transmitter, single receiver communication channel (SISO), this relationship is represented rather easily with the equation below [34]:

$$R_x = Gain * T_x * AWGN \quad (4)$$

In the Figure 10 equation, the received channel is represented as a function of antenna gain, the transmitted signal T_x, and arbitrary white Gaussian noise (AWGN). For MIMO systems, multiple transmitters use the same portion of frequency spectrum. In a traditional channel, this causes interference, and the receiver observes a signal that is a product of both transmitted signals. However, in MIMO systems, signal processing is used to reconstruct each of the transmitted streams and decode them individually. In general, this is implemented more easily when multiple receiver antennae are used. Fundamentally, this step of signal processing requires the receiver to estimate several basic characteristics of the transmitter and physical channel. These characteristics include gain, phase, and multipath effects. To generalize this relationship, each transmitted channel description is represented by a single variable, h. Thus, the system can be described with a channel model represented by the equation below [36]:

$$r = hs + n \quad (5)$$

Where **r** denotes the received signal, **s** is transmitted signal, **h** denotes the channel gain vector and **n** denotes the noise vector.

4.5 MIMO communication block diagram

The block diagram of the proposed system is shown in Fig. 4.3. Coding theory consists of two aspects: (1)to ensure the reliability of digital information transmission and processing that is error control coding, also known as channel coding;(2) to improve the effectiveness of digital information transmission, storage and processing ,that is source coding. The relationship between the two is shown in Fig. 4.3.The explanation of this block diagram is given below:

4.5.1 Line Encoder

The Line coder converts the data in bipolar NRZ form. In telecommunication, a non-return-to-zero (NRZ) line code is a binary code in which 1's are represented by one

significant condition (usually a positive voltage) and 0s are represented by some other significant condition (usually a negative voltage), with no other neutral or rest condition. The bipolar NRZ data is then encoded by outer channel coder.

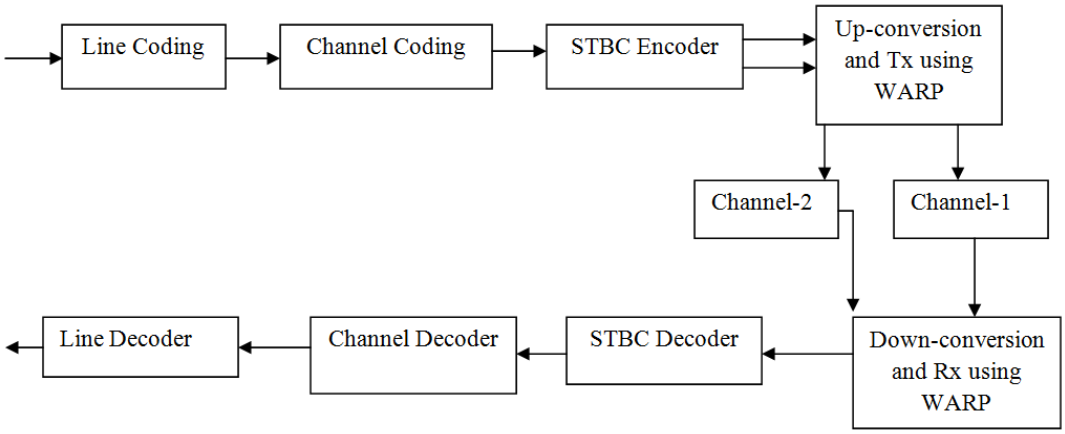

Figure 4.3 Block Diagram of Proposed System

4.5.2 Channel coding

Channel coding is a technique used for controlling errors in data transmission over unreliable or noisy communication channels [11]. The central idea is the sender encodes their message in a redundant way by using an error-correcting code (ECC). The redundancy allows the receiver to detect a limited number of errors that may occur anywhere in the message, and often to correct these errors without retransmission. FEC gives the receiver the ability to correct errors without needing a reverse channel to request retransmission of data, but at the cost of a fixed, higher forward channel bandwidth. FEC is therefore applied in situations where retransmissions are costly or impossible, such as when broadcasting to multiple receivers in multicast. FEC processing in a receiver may be applied to a digital bit stream or in the demodulation of a digitally modulated carrier. FEC is accomplished by adding redundancy to the transmitted information using a predetermined algorithm.

The two main categories of FEC codes are block codes and convolutional codes. Block codes work on fixed-size blocks (packets) of bits or symbols of predetermined size but Convolutional codes can work on bit or symbol streams of arbitrary length. There are many types of block codes, but among the classical ones the most notable is hamming codes, because of its widespread use as memory erasers in computers. Hamming ECC is commonly used to correct NAND flash memory errors. This provides single-bit error correction and 2-bit error detection. Hamming codes are only suitable for more reliable single level cell (SLC) NAND.

Classical block codes are usually implemented using hard-decision algorithms which mean that for every input and output signal a hard decision is made whether it corresponds to a one or a zero bit.

4.5.2.1 Hamming Channel Code

In telecommunication, Hamming codes are a family of linear error-correcting codes that generalize the Hamming (7,4) code invented by Richard Hamming in 1950. Hamming codes can detect up to two and correct up to one bit errors. By contrast, the simple parity code cannot correct errors, and can detect only an odd number of errors. Hamming codes are special in that they are perfect codes, that is, they achieve the highest possible rate for codes with their block length and minimum distance 3.

Because of the simplicity of Hamming codes, they are widely used in computer memory (ECC memory). In this context, one often uses an extended Hamming code with one extra parity bit. Extended Hamming codes achieve a distance of 4, which allows the decoder to distinguish between the situation in which at most one bit error occurred and the situation in which two bit errors occurred. In this sense, extended Hamming codes are single-error correcting and double-error detecting, and often referred to as **SECDED.**

For the purposes of Hamming codes, two **Hamming matrices** can be defined: the **code generator matrix G** and the **parity-check matrix H.** The size of generator matrix is [n, k] means it includes 7 rows and 4 columns. The size of parity check matrix is [n-k, n] means it includes 3 rows and 7 columns. The 4 data bits assembled as a vector **D** is pre-multiplied by **G** (i.e. G*D) and taken modulo 2 to yield the encoded value that is transmitted. The original 4 data bits are converted to 7 bits (hence the name Hamming (7, 4) with 3 parity bits added to ensure even parity. Basically the parity bits are inserted at position which are power of 2 (i.e. 2^n , n=0,1,2).

In this thesis work the hamming encoded data is transmitted using a *Space-time block coded Alamouti diversity scheme* having two transmitting and one receiving antenna, with BPSK modulation. Alamouti's transmitter diversity scheme is a simplest space time block code technique with support of two transmit antennas and an arbitrary number of receive antennas. The simplest case of Alamouti's Scheme utilizes two transmit antennas and one receive antenna [6].The same data is transmitted using *Alamouti STBC* scheme having two transmitting and two receiving antennas The samples obtained after alamouti encoder using MATLAB code are fed to the two transmitter cards.The FPGA(working at 60 MHz) implements a upconverter to convert the baseband signal to RF frequency of 2.4GHz.

The signals from the multiple antennas arrive at the receiver after travelling through two different paths. The receving modules configured with receiving antennas, receive the faded samples.the signal at receiving antenna is given as[6]:

$$r_t^i = \sum_{j=1}^{N} h_{j,i}(t) x_t^j + n_i^t \quad (6)$$

Where x^j_t is the signal transmitted from antenna i at time t. the noise n^t_i at time t is modeled as independent samples of a zero-mean complex Gaussian random variable (RV) .The coefficients hj,i(t) model fading between the jth transmit and ith receive antennas at time instant t and are assumed to be complex Gaussian random variables.

The symbol spaced receive samples are first decoded by the space-time decoder. If there is no error after reception, then the received code word **r** is identical to the transmitted code word x as shown below,

$$r = x \quad (7)$$

The receiver multiplies **H** and **r** to obtain the **syndrome** vector **Z**, in case of no error this syndrome will be a zero vector, which means no error has occurred. Otherwise, suppose a *single* bit error has occurred. Mathematically, we can write

$$r = x + e_i \quad (8)$$

Thus the above expression signifies a single bit error $\mathbf{e_i}$ in the i^{th} place. Now, if we multiply this vector by **H,**

$$Hr = H * (x + e_i) = Hx + He_i \quad (9)$$

Since **x** is the transmitted data, it is without error, and as a result, the product of **H** and **x** is zero. Thus

$$Hx + He_i = 0 + He_i = He_i \quad (10)$$

Now, the product of **H** with the i^{th} standard basis vector picks out that column of **H**, we know the error occurs in the place where this column of **H** occurs. Now syndrome is calculated as

$$Z = Hr \quad (11)$$

Once the received vector has been determined to be error-free or corrected if an error occurred then the received data has to be decoded back. Soft values generated by the space-time decoder and sent to the channel decoder for the second stage of decoding. This stage converts the data back to 4 bits from 7 bits.

4.5.3 Space Time Block Coding

Space-time block coding is a simple yet very effective means of achieving transmit diversity when other forms of diversity may be limited or non-existent, e.g., for quasi-

static fading channels. Such codes can be easily generalized to the case of multiple receive antennas as well, thus providing receive diversity in addition to transmit diversity. Furthermore, they can be decoded efficiently at the receiver by simple linear processing of the set of received signals at different receive antennas.

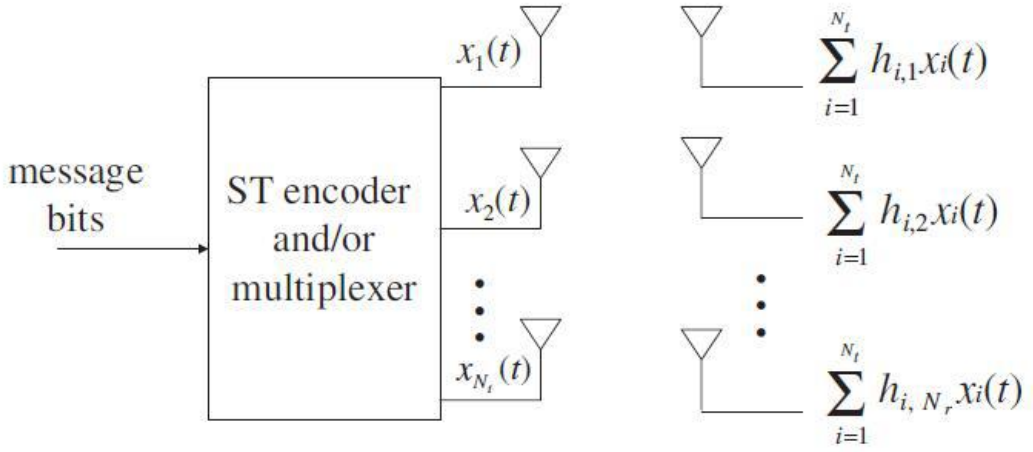

Figure 4.4 Multiple Antennas Being used for Space-Time Coding or Spatial Multiplexing

Space–time block coding is a technique used in wireless communications to transmit multiple copies of a data stream across a number of antennas and to exploit the various received versions of the data to improve the reliability of data-transfer. The fact that the transmitted signal must traverse a potentially difficult environment with scattering, reflection, refraction and so on and may then be further corrupted by thermal noise in the receiver means that some of the received copies of the data will be 'better' than others. This redundancy results in a higher chance of being able to use one or more of the received copies to correctly decode the received signal. In fact, space–time coding combines *all* the copies of the received signal in an optimal way to extract as much information from each of them as possible.

4.5.3.1 Alamouti Code

Alamouti invented the simplest of all the STBCs in 1998, although he did not coin the term "space–time block code" himself. It was designed for a two-transmit antenna system and has the coding matrix:

$$C_2 = \begin{bmatrix} c_1 & c_2 \\ -c_2^* & c_1^* \end{bmatrix} \quad (12)$$

where * denotes complex conjugate.

It is a rate-1 code as it takes two time-slots to transmit two symbols. The bit-error rate (BER) of this STBC is equivalent to 2nR branch maximal ratio combining (MRC). This is

a result of the perfect orthogonality between the symbols after receive processing, there are two copies of each symbol transmitted and nR copies received.

This is a very special STBC. It is the **only** orthogonal STBC that achieves rate-1. That is to say that it is the only STBC that can achieve its full diversity gain without needing to sacrifice its data rate. Strictly, this is only true for complex modulation symbols. Since almost all constellation diagrams rely on complex numbers however, this property usually gives Alamouti's code a significant advantage over the higher-order STBCs even though they achieve a better error-rate performance.

4.6 Image Transmission Principle

Greyscale image is a range of shades of gray without apparent color. The darkest possible shade is black, which is the total absence of transmitted or reflected light. The lightest possible shade is white, the total transmission or reflection of light at all visible. The different shades made a pixel value. These values are represented by decimal values. For the transmission the pixel values of image are obtained using MATLAB. These values are represented by 108*108 matrix of decimal values with minimum value 0 and maximum value of 255. Each decimal value represents one pixel. For transmission the decimal values were converted to binary bits, where each decimal value is represented by 8 bits. Now each pixel of image is represented by 8 binary bits of data. The dimensions of new matrix is now 108*864 bits. This 2D matrix is converted to 1D vector of size 1*93312.For the transmission this binary data is fed to the Alamouti encoder, using MATLAB code. After Alamouti encoding the data is fed to FPGA on WARP test bed for up-conversion (converting base band signal to RF signal), and then transmitted through transmitter antennas. The receiving antenna receives the faded data and stores this data in the receiver buffer and FPGA converts this data back to baseband signal. The size of this received data is [1*93312].The binary values (baseband signal) are processed in MATLAB now and converted back to the decimal values. Where 8 bits of binary data are encoded in one decimal value. The size of the new vector is now [1x11664].This vector is converted back to 108x108 matrix. This matrix represents the reconstructed image. Two performance metrics are there to evaluate the quality of the received image which are described below:

(a) Q- Index

If two images F and *G* are considered as a matrices with '*M'* column and '*N'* rows containing pixel values $F[i,j]$, $G[i,j]$, respectively ($0 \geq i>M$, $0 \geq j>N$), the universal image quality index *Q* as proposed in [6] may be calculated as a product of three components:

$$Q = \frac{\sigma_{fg}}{\sigma_f \sigma_g} * \frac{2(F_{bar})(G_{bar})}{(F_{bar})\text{^}2+(G_{bar})\text{^}2} * \frac{2\sigma_f \sigma_g}{(\sigma_f)\text{^}2+(\sigma_g)\text{^}2} \quad (13)$$

Where

$$F_{bar} = \frac{1}{MN}\sum_{i=1}^{M}\sum_{j=1}^{N} F(i,j) \quad (14)$$

$$G_{bar} = \frac{1}{MN}\sum_{i=1}^{M}\sum_{j=1}^{N} G(i,j) \quad (15)$$

$$\sigma_{fg} = \frac{1}{M+N-1}\sum_{i=1}^{M}\sum_{j=1}^{N}(F_{i,j} - F_{bar})(G_{i,j} - G_{bar}) \quad (16)$$

$$\sigma_f^2 = \frac{1}{M+N-1}\sum_{i=1}^{M}\sum_{j=1}^{N} F_{i,j} - F_{bar} \quad (17)$$

$$\sigma_g^2 = \frac{1}{M+N-1}\sum_{i=1}^{M}\sum_{j=1}^{N} G_{i,j} - G_{bar} \quad (18)$$

The first component σ_{fg} in equation (13), is the correlation coefficient, which measures the degree of linear correlation between images *F* and *G* .It varies in the range [-1, 1].$\sigma_f{}^2$, $\sigma_g{}^2$Represent the standard deviation. The second component, with a value range of [0, 1], measures how close the mean luminance is between images or it represents the mean distortion. Where F_{bar} and G_{bar} are the mean values. The third component measures how similar the contrasts of the images are or it measures the variance distortion. The value range for this component is also [0, 1].The range of values for the index *Q* is **[-1, 1].** The best value 1 is achieved if and only if the images are identical.

(b) PSNR

The PSNR is the most commonly used as a measure of quality of reconstruction of lossy image. The signal in this case is the original data. When comparing reconstructed images it is used as an approximation to human perception of reconstruction quality, therefore in some cases one reconstruction may appear to be closer to the original than another, even though it has a lower PSNR (a higher PSNR would normally indicate that the reconstruction is of higher quality). The PSNR value is measured for the different values of signal to noise ratio for both1x1 and 2x1 configurations.

It is most easily defined via the Mean Squared Error (**MSE**) which for two MxN monochrome images and G where one of the images is considered a noisy approximation of the other is defined as [32]:

$$MSE = \frac{1}{MN}\sum_{i=1}^{M}\sum_{j=1}^{N}[F_{i,j} - G_{i,j}]^2 \quad (19)$$

The PSNR is defined as:

$$PSNR = 10 * log_{10} \left[\frac{maximumvalue^{\ 2}}{MSE} \right] \text{ or} \quad (20)$$

$$PSNR = 20 * log_{10} \left[\frac{MaximumValue}{\sqrt{MSE}} \right] \quad (21)$$

Here, maximum value is the maximum possible pixel value of the image. When the pixels are represented using 8 bits per sample, this is *255*.Acceptable values of PSNR for wireless transmission quality loss are considered to be about *20 dB to 25 dB*. When the two images (transmitted and received) are identical, the MSE will be zero, for this value the PSNR is undefined.

CHAPTER 5

SIMULATION PARAMETERS AND DETAILS

M-PSK modulation technique has been employed on WARP test bed and comparison has been made between Bit Error Rate and Base Band gain. The SISO, MISO, MIMO configuration has been taken into account for transmission and reception of image.

5.1 Simulation Details

The parameters used in transmission of image are shown in table 5.1 below

TABLE 5.1 Simulation parameters

Transmission Delay	**0 to 16384**
Transmission Length	0 to 16384-Transmission delay
Carrier Channel	1 to14
Base Band Transmitter Gain	0 to 3
RF Transmitter Gain	0 to 63
Base Band Receiver Gain	0 to 31
RF Receiver Gain	1 to 3
Transmission Mode	0 for single transmission 1 for continuous transmission
Gain Control	0 to enable automatic gain control 1 to enable manual gain control

5.2 Flow chart of working model

Below is the description of step by step procedure of process which takes place outside and inside WARP FPGA board. There are basically two interfacing cables which results in proper signal flow through PC to WARP FPGA and vice-versa. One is Ethernet cable provides a speed of 100 Mbps and other is JTAG cable. JTAG cable provides the compatibility between host PC and WARP FPGA board.

Initialisation of various global parameters like RF and BB gains of transmitter and receiver is done. Socket handling and nodes are also initialized as global parameter. Along with these parameters such as transmission length i.e. TxLength, transmitter delay i.e. TxDelay, Carrier channel are also initialized. For continuous transmission the transmission mode has to be set to value 1 and the transmitting antenna continues to transmit the samples until the antenna is disabled manually by the user, otherwise it is set to value 0 in case of single bit transmission. Parameters such as manual gain control and

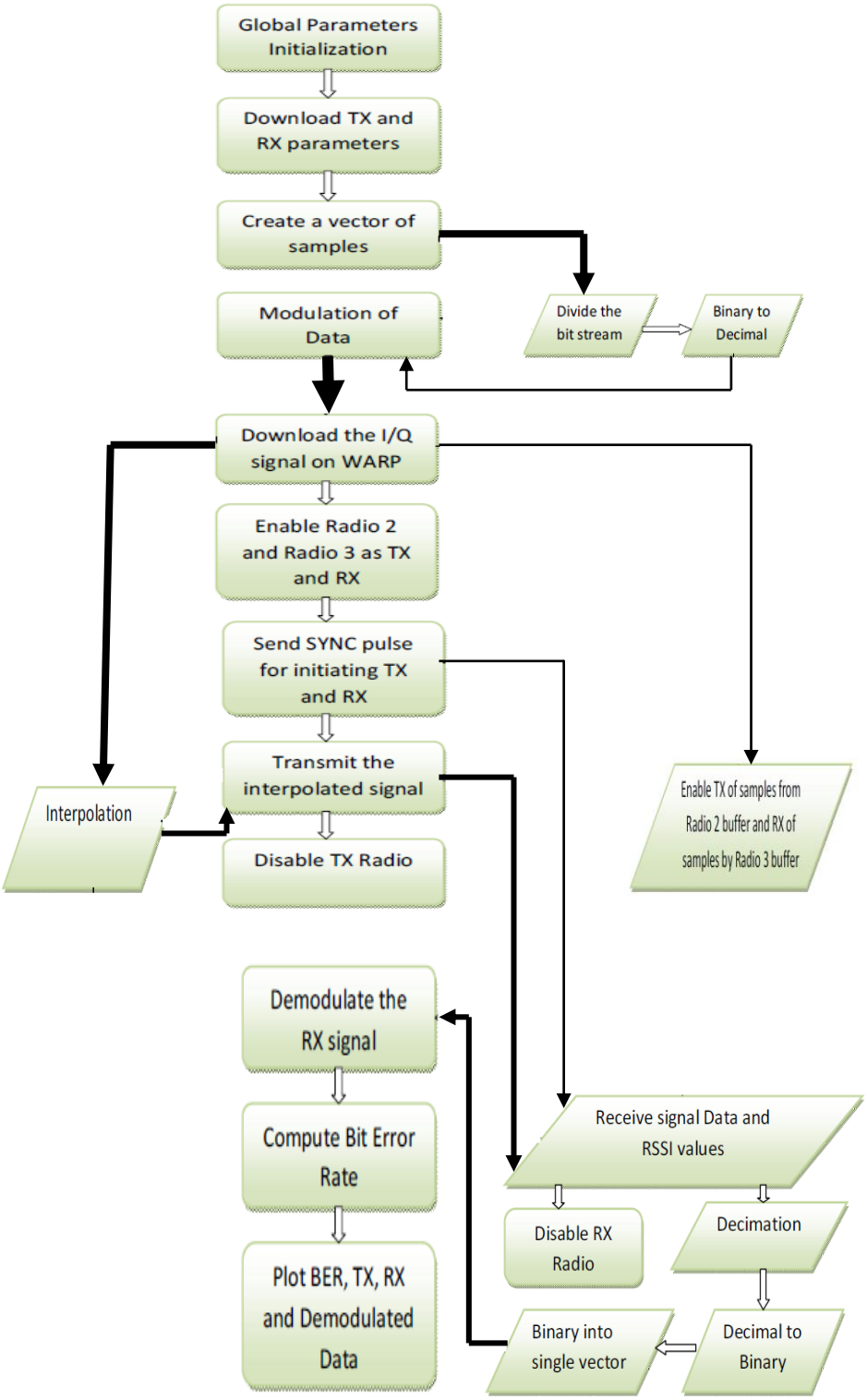

Figure 5.1 Flow Chart of Procedure

Automatic gain control can also be set depending upon the requirement. These all parameters are downloaded to the transmitter and receiver node's buffer through interconnecting cables. The signal to be transmitted is generated using MATLAB as a row vector. Out of the available 4 radio cards it is up to the user to make any of the radio

board as transmitter or receiver by setting proper parameters in MATLAB code. For the transmission the transmitter and receiver radio cards buffers has to be enabled first. For the reception of signal the receiver radio card must receive a SYNC pulse. Reception will take place only when receiver radio card will receive a SYNC pulse. It shows that synchronisation is very important so that samples are received at the same time at which they are transmitted.

Chapter 6
RESULTS AND DISCUSSIONS

Two modulation techniques have been implemented for 1x1, 2x1, 2x2 systems. Bit error rate (BER) for modulation scheme using FPGA based Wireless Access Research Platform test bed has been compared. The hardware used is responsible for real time analysis of different modulation techniques under natural environment. FPGA used is Virtex-4 on which real time implementation of various designs are possible such as designs using system generator, Power PC, and programming through language like MATLAB. However results shown are through the source code running in MATLAB. The code comprises of a number of standard functions responsible for correct operation of a few modules of WARP board which are responsible for desired and effective functioning of intermediate nodes used for signal processing. Daughter cards work on the basis of these functions such as the socket and node initialisation, radio boards association, initialisation of global parameters from WARP lab, enabling and disabling of transmitter and receiver radio boards and their associated antennas etc. The variable parameter in the design code is transmitting signal baseband gain, which vary over each iteration to study the performance of modulation techniques in lieu of BER. The modulation techniques used are M-PSK and M-QAM. The results obtained for these techniques consist of transmitting row vector.

WARP board has transmitter radio board with a variation of three values of transmitter base band gain i.e. from 1 to 3.So for each value of this gain bit error rate is calculated and it will be seen below that which modulation technique has better performance than other. It is also shown that the performance of modulation techniques varies with the order of modulation. Also the usage of number of bits per symbol effect the capacity and interference of these techniques. Comparison has been made between the simulation of modulation techniques with and without WARP FPGA board.

6.1 Performance comparison of 1X1, 2x1, 2x2 systems for transmission of grey scale image using BPSK

For the implementation of proposed system a grey scale image of ‘lennags’ is taken. The pixel values of image are obtained using MATLAB. These values are represented by 108x108 matrix of decimal values with minimum value 0 and maximum value of 255. Each decimal value represents one pixel. For our experiment the decimal values were

converted to binary bits, where each decimal value is represented by 8 bits. Now each pixel of image is represented by 8 binary bits of data. The dimensions of new matrix is now 108x864.This 2D matrix is converted to 1D vector of size 1x93312.This binary data is fed to the Alamouti encoder ,using MATLAB code. After Alamouti encoding the data is fed to FPGA on WARP test bed for up-conversion (converting base band signal to RF signal), and then transmitted through transmitter antennas. The receiving antenna receives the faded data and stores this data in the receiver buffer and FPGA converts this data back to baseband signal. The size of this received data is [1x93312]. The binary values (baseband signal) are processed in MATLAB now and converted back to the decimal values. Where 8 bits of binary data are encoded in one decimal value. The size of the new vector is now [1x11664].This vector is converted back to 108x108 matrixes. This matrix represents the reconstructed image. Figure 6.1 (a) shows the transmitted using BPSK modulation. This image was first transmitted using only one transmitter and one receiver on WARP test bed. The transmitted and received images are shown in figure 6.1. The values obtained for PSNR and Q index is shown in table 6.1 for this configuration.

Figure 6.1 (a) Transmitted image (1x1) using BPSK modulation

Figure 6.1 (b) Received image (1x1) (SNR=1 dB, PSNR=13.8877 dB)

Figure 6.1 (c) Received image (1x1) (SNR=3 dB, PSNR=15.3298dB)

Figure 6.1 (d) Received image (1x1) (SNR=5 dB, PSNR=14.9546dB)

Figure 6.1 (e) Received image (1x1) (SNR=6 dB, PSNR=17.8502dB)

Figure 6.1 (f) Received image (1x1) (SNR=7 dB, PSNR=18.2804dB)

Figure 6.1 (g) Received image (1x1) (SNR=8 dB, PSNR=19.3317dB)

Figure 6.1 (h) Received image (1x1) (SNR=9 dB, PSNR=20.1415dB)

For different values of SNR the PSNR and Q-index of received image is also calculated. The calculated values are shown in table 6.1.

TABLE 6.1 Performance of BPSK for 1x1 configuration

SNR (dB)	PSNR (dB)	Q-INDEX
1	13.8877	0.8410
2	14.4392	0.8577
3	15.3298	0.8736
4	15.8451	0.8900
5	16.7423	0.9103
6	17.8502	0.9210
7	18.2804	0.9510
8	19.3317	0.9699
9	20.4015	0.9750

The same image of ‘ Lennags’ is transmitted using 2x1 configuration, means using two transmitter and only one receiver on WARP test bed. For different values of SNR, the

values of PSNR and Q-index are calculated. The transmitted and received images are shown in figure 6.2.

Figure 6.2 (a) Transmitted image (2x1) using BPSK modulation

Figure 6.2 (b) Received image (2x1) (SNR=1 dB, PSNR=14.9546dB)

Figure 6.2 (c) Received image (2x1) (SNR=3 dB, PSNR=17.2246dB)

Figure 6.2 (d) Received images (2x1) (SNR=5 dB, PSNR=19.6950dB)

Figure 6.2 (e) Received image (2x1) (SNR=6dB, PSNR=20.9395dB)

Figure 6.2 (f) Received images (2x1) (SNR=7dB, PSNR=22.2570dB)

Figure 6.2 (g) Received image (2x1) (SNR=8dB, PSNR=24.1252dB)

Figure 6.2 (h) Received images (2x1) (SNR=9dB, PSNR=25.4945dB)

For different values of SNR the PSNR and Q-index of received image is also calculated. The calculated values are shown in table 6.2.

TABLE 6.2 Performance of BPSK for 2x1 configuration

SNR (dB)	PSNR (dB)	Q-INDEX
1	14.9564	0.8568
2	15.9463	0.8786
3	17.2263	0.8948
4	18.2878	0.9112
5	19.6950	0.9363
6	20.9395	0.9532
7	22.2507	0.9795
8	24.1252	0.9850
9	25.4945	0.9920

The same image of ' Lennags' is transmitted using 2x2 configuration, means using two transmitter and two receivers on WARP test bed. For different values of SNR, the values of PSNR and Q-index are calculated. The transmitted and received images are shown in figure 6.3.

Figure 6.3 (a) Transmitted image (2x2) using BPSK modulation

Figure 6.3 (b) Received images (2x2) (SNR=1 dB, PSNR=16.0251 dB)

Figure 6.3 (c) Received images (2x2) (SNR=3 dB, PSNR=19.1228dB)

Figure 6.3 (d) Received images (2x2) (SNR=5 dB, PSNR=22.6480dB)

Figure 6.3 (e) Received images (2x2) (SNR=6 dB, PSNR=24.0280dB)

Figure 6.3 (f) Received images (2x2) (SNR=7 dB, PSNR=26.2210dB)

Figure 6.3 (g) Received images (2x2) (SNR=8 dB, PSNR=28.9187 dB)

Figure 6.3 (h) Received images (2x2) (SNR=9 dB, PSNR=30.5575 dB)

For different values of SNR the PSNR and Q-index of received image is also calculated. The calculated values are shown in table 6.3.

TABLE 6.3 Performance of BPSK for 2x2 configuration

SNR (dB)	PSNR (dB)	Q-INDEX
1	16.0251	0.8726
2	17.4534	0.8995
3	19.1228	0.9160
4	20.7305	0.9324
5	22.6480	0.9523
6	24.0288	0.9550
7	26.2210	0.9810
8	28.9187	0.9870
9	30.5875	0.9925

6.1.1 The Comparison of PSNR values for 1x1, 2x1, 2x2 configurations for BPSK modulation

Fig 6.4 indicates the plot of Base Band gain (x-axis) and PSNR (y-axis). The comparison has been done among for 1x1(green curve), 2x1(blue curve) and 2x2(red curve) systems.

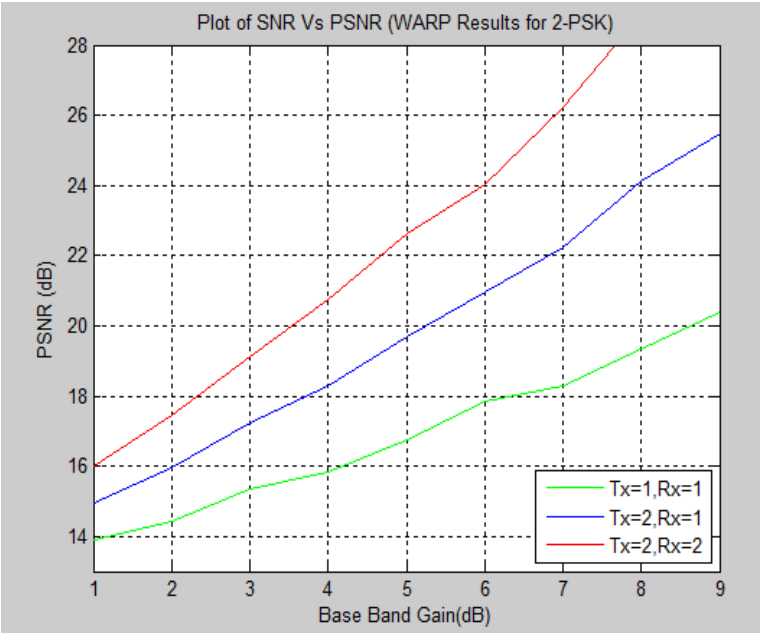

Figure 6.4 Plot of Base Band Gain vs. PSNR for BPSK modulation

From theory the minimum acceptable value of PSNR for wireless transmission quality loss should be about ***20 dB to 25 dB***. The results obtained from WARP test bed shows that when the image is transmitted using only one transmitted and one receiving antenna the minimum acceptable value of PSNR is obtained at SNR of 9 dB, but when the same image is transmitted using two transmitter and one receiving antenna, keeping all other parameters same then this value of PSNR is obtained at 6 dB. The same image when transmitted using two transmitting and two receiving antennas then the minimum acceptable value of PSNR is obtained at SNR of 4 dB. It means there is 3 dB improvement in SNR while switching from 1x1 configuration to 2x1 and 2 dB improvement in SNR while switching from 2x1 configuration to 2x2 system.

6.1.2 The Comparison of Q-Index for different values of Base Band gain for 1x1, 2x1, 2x2 configurations for BPSK modulation

Fig 6.5 indicates the plot of Base Band Gain (x-axis) and Q-index (y-axis). The comparison has been done among for 1x1(blue curve), 2x1(green curve) and 2x2(red curve) systems. The results obtained from WARP test bed shows that when the image is transmitted using only one transmitted and one receiving antenna the 0.87 value of Q-index is obtained at SNR of 3 dB, but when the same image is transmitted using two transmitter and one receiving antenna, keeping all other parameters same then this value of Q-index is obtained at 2 dB. The same image when transmitted using two transmitting and two receiving antennas then the minimum acceptable value of Q-index is obtained at SNR of 1 dB.

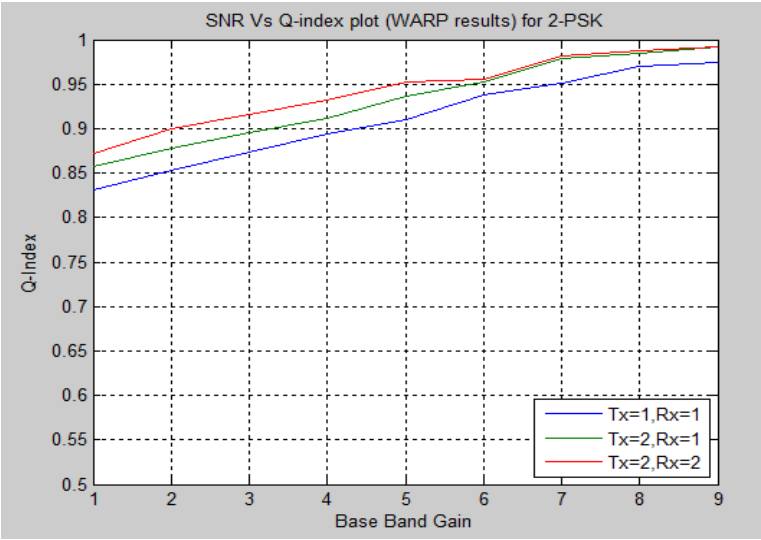

Figure 6.5 Plot Base Band Gain vs. Q-Index for BPSK modulation

It means there is 1 dB improvement in SNR while switching from 1x1 configuration to 2x2 for the transmission of same image.

6.1.3 The Comparison of BER values for 1x1, 2x1, 2x2 configurations for BPSK modulation

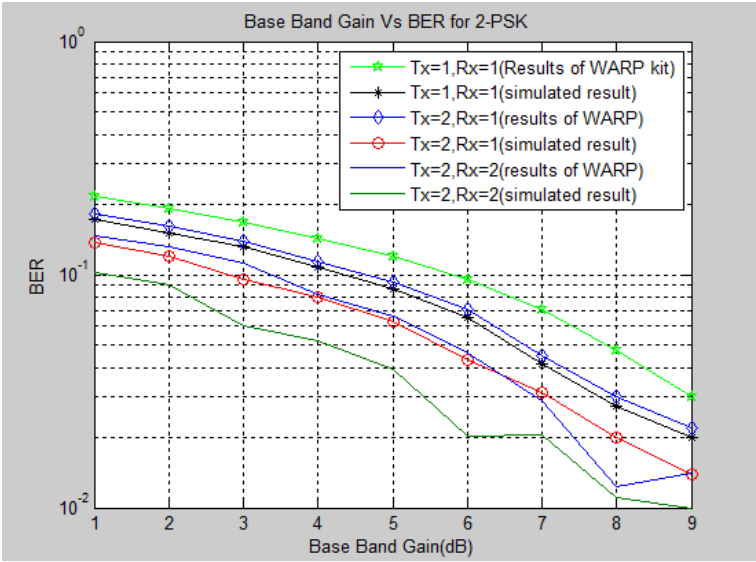

Figure 6.6 Plot of Base Band Gain vs. BER for BPSK modulation

Figure 6.6 indicates the plot of Base Band gain (x-axis) and BER (y-axis).This plot is obtained after transmission of "Lennags" image using BPSK modulation technique for three different configurations. The 3 out of 6 curves in this plot is for simulated results and other three are results obtained after implementation on WARP test bed for BPSK modulation. From the figure above it is clear that BER of 10-1 is obtained at SNR of 6.0 dB for 1x1system, at SNR of 4.8 dB for 2x1system and at SNR of 3.6 dB for 2x2 system. So there is improvement of 1.2 dB if we are switching from 1x1 configuration to 2x1 and

improvement of 1.2 dB if we are switching from 2x1 configuration to 2x2 for transmission of “Lennags” image through WARP test bed.

6.2 Performance comparison of 1X1, 2x1, 2x2 systems for transmission of grey scale image using QPSK

The image of ‘Lennags’ is transmitted using 1x1 configuration, but for QPSK modulation here. For different values of SNR, the values of PSNR and Q-index are calculated. The transmitted and received images are shown in figure 6.7.

Figure 6.7 (a)Transmitted Image (1x1) using QPSK modulation

Figure 6.7 (b) Received images (1x1) (SNR=15 dB, PSNR=17.4777 dB)

Figure 6.7 (c) Received images (1x1) (SNR=17 dB, PSNR=19.9347 dB)

Figure 6.7 (d) Received images (1x1) (SNR=18 dB, PSNR=20.6890 dB)

Figure 6.7 (e) Received images (1x1) (SNR=19 dB, PSNR=21.6238 dB)

Figure 6.7 (f) Received images (1x1) (SNR=20 dB, PSNR=22.5483 dB)

For different values of SNR the PSNR and Q-index of received image is also calculated. The calculated values are shown in table 6.4.

TABLE 6.4 Performance of QPSK for 1x1 Configuration

SNR (dB)	PSNR (dB)	Q-INDEX
14	16.5939	0.4205
15	17.4777	0.5053
16	18.6911	0.5602
17	19.9347	0.6506
18	20.6890	0.7342
19	21.6238	0.8365
20	22.5483	0.8460

The same image of ‘ Lennags’ is transmitted using 2x1 configuration, means using two transmitter and only one receiver on WARP test bed with QPSK modulation. For different values of SNR, the values of PSNR and Q-index are calculated. The transmitted and received images are shown in figure 6.8.

Figure 6.8 (a)Transmitted Image (2x1)

Figure 6.8 (b) Received images (2x1) (SNR=14 dB, PSNR=17.6626 dB)

Figure 6.8 (c) Received images (2x1) (SNR=15 dB, PSNR=18.9848 dB)

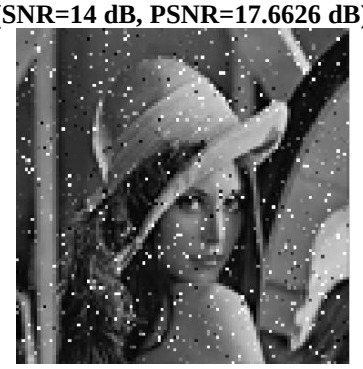

Figure 6.8 (d) Received images (2x1) (SNR=16 dB, PSNR=20.5876 dB)

Figure 6.8 (e) Received images (2x1) (SNR=17 dB, PSNR=21.7338 dB)

Figure 6.8 (f) Received images (2x1) (SNR=18 dB, PSNR=23.6147 dB)

For different values of SNR the PSNR and Q-index of received image is also calculated. The calculated values are shown in table 6.5.

TABLE 6.5 Performance of QPSK for 2x1 Configuration

SNR (dB)	PSNR (dB)	Q-INDEX
14	17.6626	0.4363
15	18.9848	0.5262
16	20.5876	0.5814
17	21.7338	0.6718
18	23.6417	0.7602
19	24.7131	0.8687
20	25.6380	0.8745

The same image of ‘ Lennags’ is transmitted using 2x2 configuration, means using two transmitter and two receivers on WARP test bed using QPSK modulation. For different values of SNR, the values of PSNR and Q-index are calculated. The transmitted and received images are shown in figure 6.9.

Figure 6.9 (a)Transmitted Image (2x2)

Figure 6.9 (b) Received images (2x2) (SNR=14 dB, PSNR=18.7313 dB)

Figure 6.9 (c) Received images (2x2) (SNR=16 dB, PSNR=22.4841 dB)

Figure 6.9 (d) Received images (2x2) (SNR=18 dB, PSNR=26.5944 dB)

Figure 6.9 (e) Received images (2x2) (SNR=19 dB, PSNR=27.8024 dB)

By using two transmitting and two receiving antennas and for different values of Base Band gain the PSNR and Q-index of received image is also calculated. The calculated values are shown in table 6.6.

TABLE 6.6 Performance of QPSK for 2x2 configuration

SNR (dB)	PSNR (dB)	Q-INDEX
14	18.7313	0.4521
15	20.4919	0.5471
16	22.4841	0.6026
17	23.5329	0.6930
18	26.5944	0.7762
19	27.8024	0.8705
20	28.7277	0.8760

6.2.1 The Comparison of PSNR for Different values of Base band Gain for 1x1, 2x1, 2x2 configurations for QPSK modulation

Fig 6.10 indicates the plot of Base Band gain (x-axis) and PSNR (y-axis). The comparison has been done among for 1x1(green curve), 2x1(blue curve) and 2x2(red curve) systems. From theory the minimum acceptable value of PSNR for wireless transmission quality loss

should be about ***20 dB to 25 dB***. The results obtained from WARP test bed shows that when the image is transmitted using only one transmitted and one receiving antenna the minimum acceptable value of PSNR is obtained at SNR of 18 dB, but when the same image is transmitted using two transmitter and one receiving antenna, keeping all other parameters same then this value of PSNR is obtained at 16 dB. The same image when transmitted using two transmitting and two receiving antennas then the minimum acceptable value of PSNR is obtained at SNR of 15 dB.

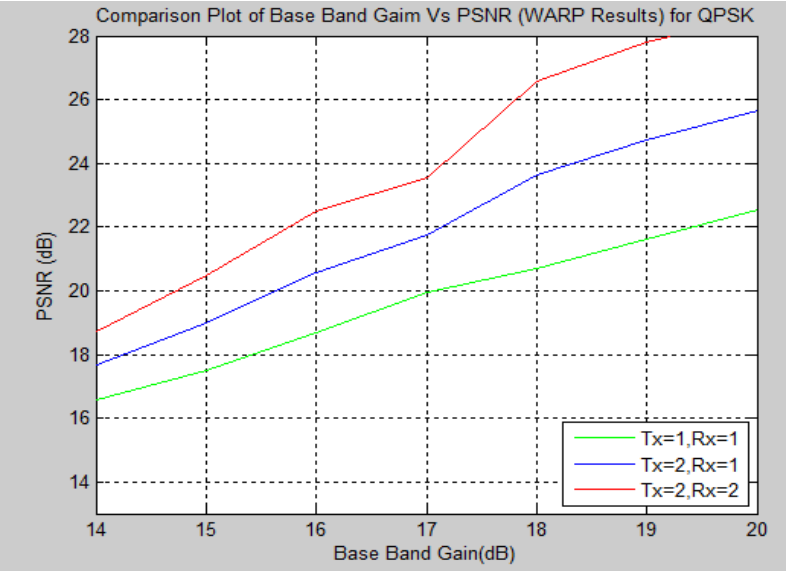

Figure 6.10 Plot of Base Band Gain vs. PSNR for QPSK modulation

It means there is 2 dB improvement in base band gain while switching from 1x1 configuration to 2x1 and 1 dB improvement in base band gain while switching from 2x1 configuration to 2x2 system.

6.2.2 The Comparison of Q-Index for different values of Base Band gain for 1x1, 2x1, 2x2 configurations for QPSK modulation

Fig 6.11 indicates the plot of Base Band Gain (x-axis) and Q-index (y-axis). The comparison has been done among for 1x1(blue curve), 2x1(green curve) and 2x2(red curve) systems. The results obtained from WARP test bed shows that when the image is transmitted using only one transmitted and one receiving antenna the 0.84 value of Q-index is obtained at base band gain of 20 dB, but when the same image is transmitted using two transmitter and one receiving antenna, keeping all other parameters same then this value of Q-index is obtained at 19 dB. The same image when transmitted using two transmitting and two receiving antennas then the minimum acceptable value of Q-index is obtained at SNR of 18 dB. It means there is 2 dB improvement in base band gain while switching from 1x1 configuration to 2x2 for the transmission of same image.

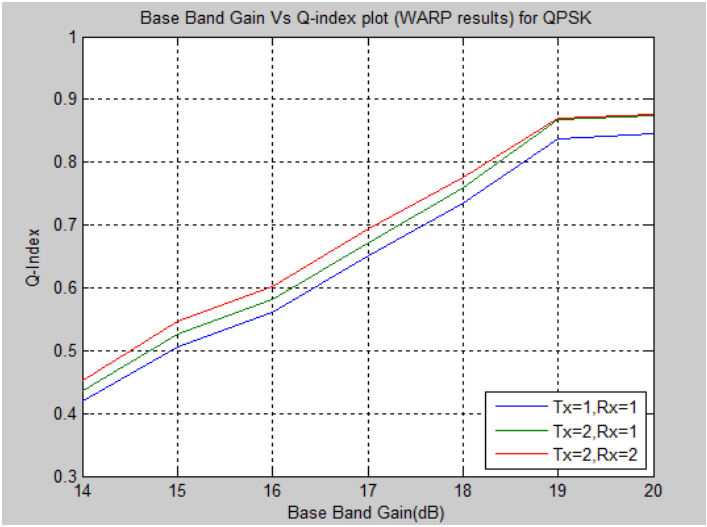

Figure 6.11 Plot of Base Band Gain vs. Q-Index for QPSK modulation

6.2.3 The Comparison of BER values for 1x1, 2x1, 2x2 configurations for QPSK modulation

Figure 6.12 indicates the plot of Base Band gain (x-axis) and BER (y-axis).This plot is obtained after transmission of "Lennags" image using BPSK modulation technique for three different configurations. The 3 out of 6 curves in this plot is for simulated results and other three are results obtained after implementation on WARP test bed for BPSK modulation. From the figure above it is clear that BER of 10-1 is obtained at SNR of 8.7 dB for 1x1system, at SNR of 8.0 dB for 2x1system and at SNR of 6.8 dB for 2x2 system.

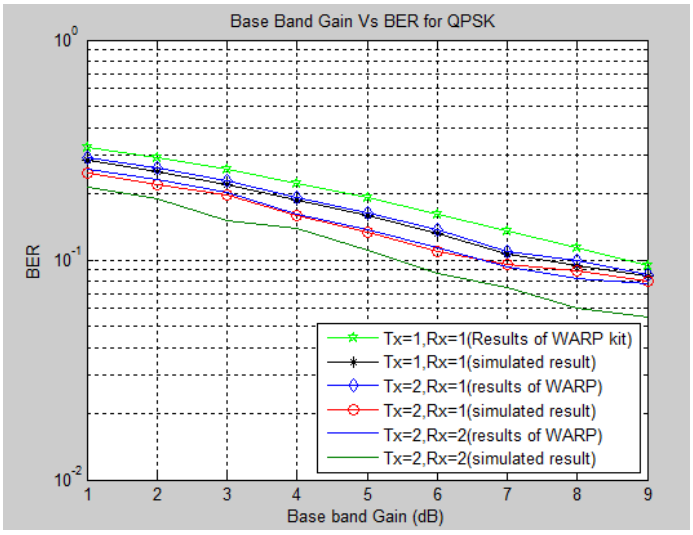

Figure 6.12 Plot of Base Band Gain vs. BER for QPSK modulation

So there is improvement of 0.7 dB in base band gain if we are switching from 1x1 configuration to 2x1 and improvement of 1.2 dB in base band gain if we are switching from 2x1 configuration to 2x2 configuration to 2x2.

6.3 Performance comparison of 1X1, 2x1, 2x2 systems for transmission of grey scale image using 2-QAM

The image of 'Lennags' is transmitted using 1x1 configuration, but for 2-QAM modulation. For different values of SNR, the values of PSNR and Q-index are calculated. The results are shown in table 6.7 below.

TABLE 6.7 Performance of 2-QAM for 1x1 Configuration

SNR (dB)	PSNR (dB)	Q-INDEX
1	13.9176	0.8110
2	14.3303	0.8337
3	15.0279	0.8536
4	15.7453	0.8743
5	16.9228	0.8903
6	17.4614	0.9179
7	18.5047	0.9310
8	19.5091	0.9499
9	20.0300	0.9550

The same image of ' Lennags' is transmitted using 2x1 configuration, means using two transmitter and only one receiver on WARP test bed with 2-QAM modulation. For different values of SNR, the values of PSNR and Q-index are calculated. These values are given in table 6.8.

TABLE 6.8 Performance of 2-QAM for 2x1 Configuration

SNR (dB)	PSNR (dB)	Q-INDEX
1	15.0909	0.8368
2	16.0651	0.8586
3	17.0881	0.8748
4	18.3490	0.8912
5	19.6907	0.9163
6	20.8557	0.9332
7	22.7461	0.9510
8	24.2753	0.9650
9	25.8425	0.9520

The same image of ' Lennags' is transmitted using 2x2 configuration, means using two transmitter and only one receiver on WARP test bed with 2-QAM modulation. For different values of SNR, the values of PSNR and Q-index are calculated. These values are given in table 6.9.

TABLE 6.9 Performance of 2-QAM for 2x2 Configuration

SNR (dB)	PSNR (dB)	Q-INDEX
1	16.2642	0.8526
2	17.7999	0.8795
3	19.6907	0.8960
4	20.9527	0.9124
5	22.4586	0.9323
6	24.2500	0.9450
7	26.9875	0.9595
8	29.0415	0.9770
9	31.655	0.9625

6.3.1 The Comparison of PSNR for Different values of Base band Gain for 1x1, 2x1, 2x2 configurations for 2-QAM modulation

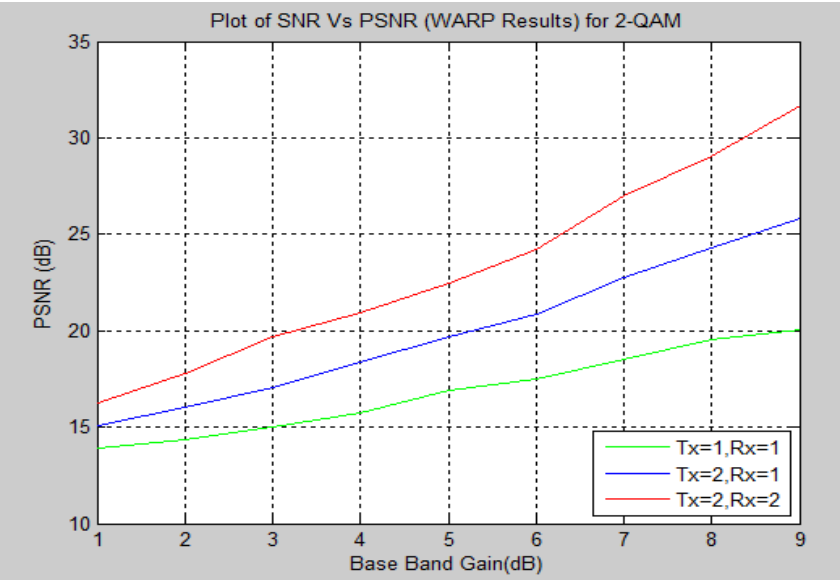

Figure 6.13 Plot of Base Band Gain vs. PSNR for 2-QAM

Fig 6.13 indicates the plot of Base Band gain (x-axis) and PSNR (y-axis). The comparison has been done among for 1x1(green curve), 2x1(blue curve) and 2x2(red curve) systems. From theory the minimum acceptable value of PSNR for wireless transmission quality loss should be about ***20 dB to 25 dB***. The results obtained from

WARP test bed shows that when the image is transmitted using only one transmitted and one receiving antenna the minimum acceptable value of PSNR is obtained at SNR of 9 dB, but when the same image is transmitted using two transmitter and one receiving antenna, keeping all other parameters same then this value of PSNR is obtained at 6 dB. The same image when transmitted using two transmitting and two receiving antennas then the minimum acceptable value of PSNR is obtained at SNR of 4 dB. It means there is 3 dB improvement in base band gain while switching from 1x1 configuration to 2x1 and 2 dB improvement in base band gain while switching from 2x1 configuration to 2x2 system.

6.3.2 The Comparison of Q-Index for Different values of Base band Gain for 1x1, 2x1, 2x2 configurations for 2-QAM

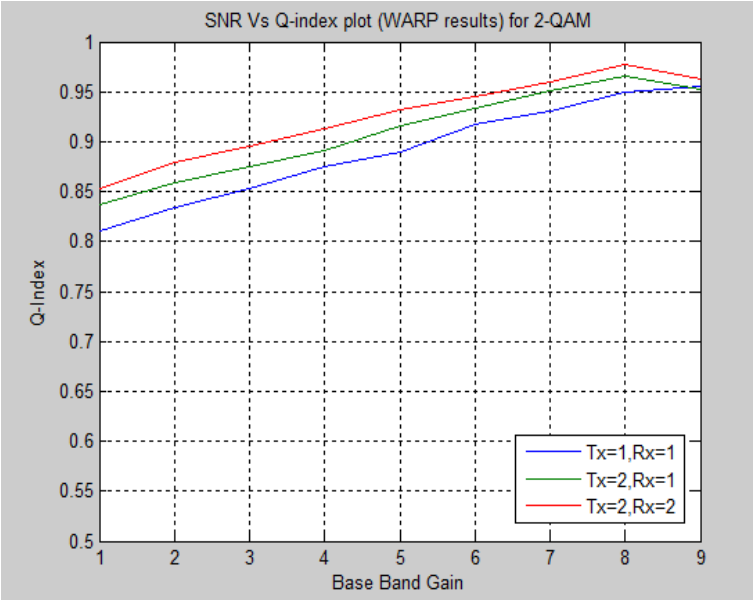

Figure 6.14 Plot of Base Band Gain vs. Q-Index for 2-QAM

Fig 6.14 indicates the plot of Base Band Gain (x-axis) and Q-index (y-axis). The comparison has been done among for 1x1(blue curve), 2x1(green curve) and 2x2(red curve) systems. The results obtained from WARP test bed shows that when the image is transmitted using only one transmitted and one receiving antenna the 0.84 value of Q-index is obtained at base band gain of 3 dB, but when the same image is transmitted using two transmitter and one receiving antenna, keeping all other parameters same then this value of Q-index is obtained at 2 dB. The same image when transmitted using two transmitting and two receiving antennas then the minimum acceptable value of Q-index is obtained at SNR of 1 dB. It means there is 2 dB improvement in base band gain while switching from 1x1 configuration to 2x2 for the transmission of same image.

6.4 Performance comparison of 1X1, 2x1, 2x2 systems for transmission of grey scale image using 4-QAM

The same image of ' Lennags' is transmitted using 1x1 configuration, means using two transmitter and only one receiver on WARP test bed with 4-QAM modulation. For different values of SNR, the values of PSNR and Q-index are calculated. These values are given in table 6.10.

TABLE 6.10 Performance of 4-QAM for 1x1 Configuration

SNR (dB)	PSNR (dB)	Q-INDEX
14	19.7091	0.4405
15	20.5701	0.5253
16	22.0459	0.5802
17	22.8050	0.6706
18	23.9511	0.7542
19	24.4150	0.8565
20	26.3596	0.8760

The same image of ' Lennags' is transmitted using 2x1 configuration, means using two transmitter and only one receiver on WARP test bed with 4-QAM modulation. For different values of SNR, the values of PSNR and Q-index are calculated. These values are given in table 6.11.

TABLE 6.11 Performance of 4-QAM for 2x1 Configuration

SNR (dB)	PSNR (dB)	Q-INDEX
14	20.8824	0.4563
15	22.3049	0.5462
16	24.1061	0.6014
17	25.4087	0.6910
18	26.7190	0.7802
19	27.8093	0.8887
20	30.6010	0.8945

The same image of ' Lennags' is transmitted using 2x2 configuration, means using two transmitter and only one receiver on WARP test bed with 4-QAM modulation. For different values of SNR, the values of PSNR and Q-index are calculated. These values are given in table 6.12.

TABLE 6.12 Performance of 4-QAM for 2x2 Configuration

SNR (dB)	PSNR (dB)	Q-INDEX
14	22.0557	0.4721
15	24.0397	0.5671
16	26.1663	0.6226
17	28.0124	0.6940
18	29.4869	0.7962
19	30.8093	0.8905
20	34.8424	0.9160

6.4.1 The Comparison of PSNR for Different values of Base band Gain for 1x1, 2x1, 2x2 configurations for 4-QAM modulation

Figure 6.15 Plot of Base Band Gain vs. PSNR for 4-QAM

Fig 6.15 indicates the plot of Base Band gain (x-axis) and PSNR (y-axis). The comparison has been done among for 1x1(green curve), 2x1(blue curve) and 2x2(red curve) systems. From theory the minimum acceptable value of PSNR for wireless transmission quality loss should be about ***20 dB to 25 dB***. The results obtained from WARP test bed shows that when the image is transmitted using only one transmitted and one receiving antenna the minimum acceptable value of PSNR is obtained at SNR of 15 dB, but when the same image is transmitted using two transmitter and one receiving antenna, keeping all other parameters same then this value of PSNR is obtained at 14 dB. The same image when transmitted using two transmitting and two receiving antennas then

the minimum acceptable value of PSNR is obtained at SNR of 13 dB. It means there is 1 dB improvement in base band gain while switching from 1x1 configuration to 2x1 and 1 dB improvement in base band gain while switching from 2x1 configuration to 2x2 system.

6.4.2 The Comparison of Q-Index for Different values of Base band Gain for 1x1, 2x1, 2x2 configurations for 4-QAM modulation

Fig 6.16 indicates the plot of Base Band Gain (x-axis) and Q-index (y-axis). The comparison has been done among for 1x1(blue curve), 2x1(green curve) and 2x2(red curve) systems. The results obtained from WARP test bed shows that when the image is transmitted using only one transmitted and one receiving antenna the 0.84 value of Q-index is obtained at base band gain of 19 dB, but when the same image is transmitted using two transmitter and one receiving antenna, keeping all other parameters same then this value of Q-index is obtained at 17.5 dB. The same image when transmitted using two transmitting and two receiving antennas then the minimum acceptable value of Q-index is obtained at SNR of 16.5 dB. It means there is 2.5 dB improvement in base band gain while switching from 1x1 configuration to 2x2 for the transmission of same image.

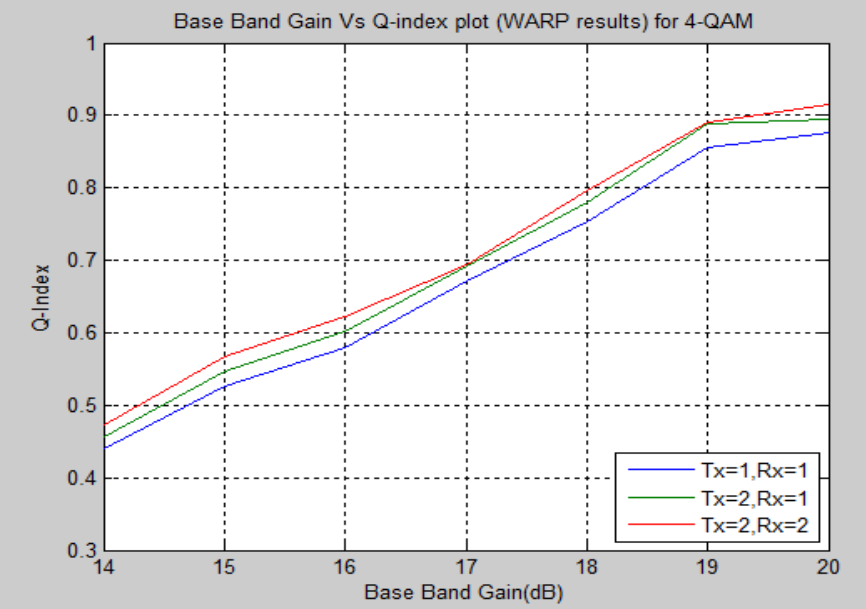

Figure 6.16 Plot of Base Band Gain vs. Q-Index for 4-QAM

6.5 Performance results for Implementation of concatenated Hamming (7, 4) Channel code and Alamouti code

Previous results were implemented on WARP test bed without using any channel coding technique. We have implemented concatenated Hamming codes and space-time block codes on Wireless Access Research Platform (WARP) hardware test bed. The

performance comparison between simulated and implemented concatenated scheme for BPSK modulation is done in terms of Bit Error Rate (BER) for different values of Signal to Noise Ratio (SNR). The obtained results here when compared with the results discussed in previous section shows that system using concatenated scheme for image transmission reduces the BER. Hamming code is used as an outer code while STBC is used as inner code. The proposed system demonstrates good error correcting capability of concatenated scheme with a diversity gain.

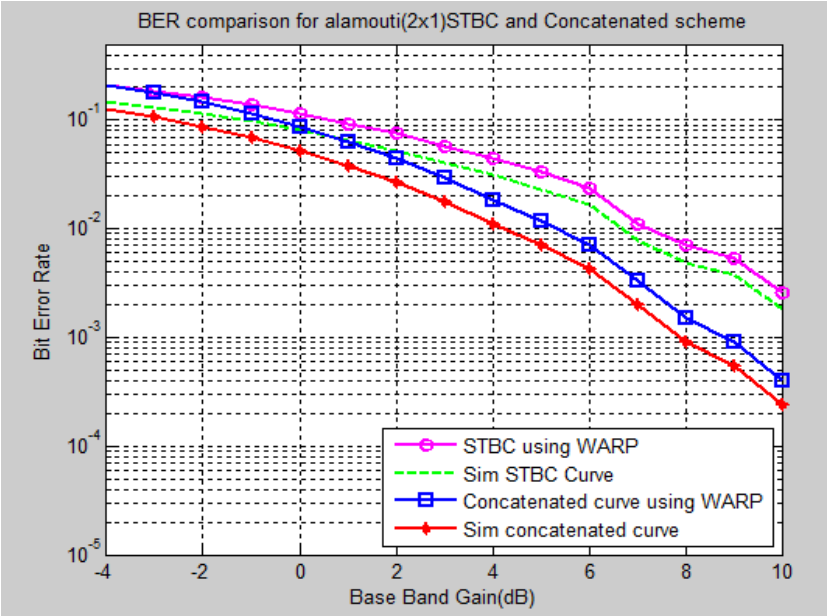

Figure 6.17 BER vs. SNR plot for 2x1 System

Figure 6.17 indicates the plot of SNR (x-axis) and BER (y-axis). The BER curves compared on this plot is for 2x1system. The comparison has been made between simulated results and the results obtained through WARP test bed. The 2 out of four curves in this plot is for simulated results (indicated by red curve and green curve).Green curve indicates the BER for data transmitted using STBC coding and red curve indicates the BER curve for data transmitted using concatenated scheme. The other 2 curves in this plot is for WARP test bed results (indicated by pink curve and blue curve).Pink curve indicates the BER for data transmitted using only STBC coding and blue curve indicates the BER curve for data transmitted using concatenated scheme.

Figure 6.18 indicates the plot of SNR (x-axis) and BER (y-axis). The BER curves compared on this plot is for 2x2system. The comparison has been made between simulated results and the results obtained through WARP test bed. The 2 out of four curves in this plot is for simulated results (indicated by red curve and green curve).Green curve indicates the BER for data transmitted using only STBC coding and red curve

indicates the BER curve for data transmitted using concatenated scheme. The other 2 curves in this plot is for WARP test bed results (indicated by pink curve and blue curve).Pink curve indicates the BER for data transmitted using only STBC coding and blue curve indicates the BER curve for data transmitted using concatenated scheme.

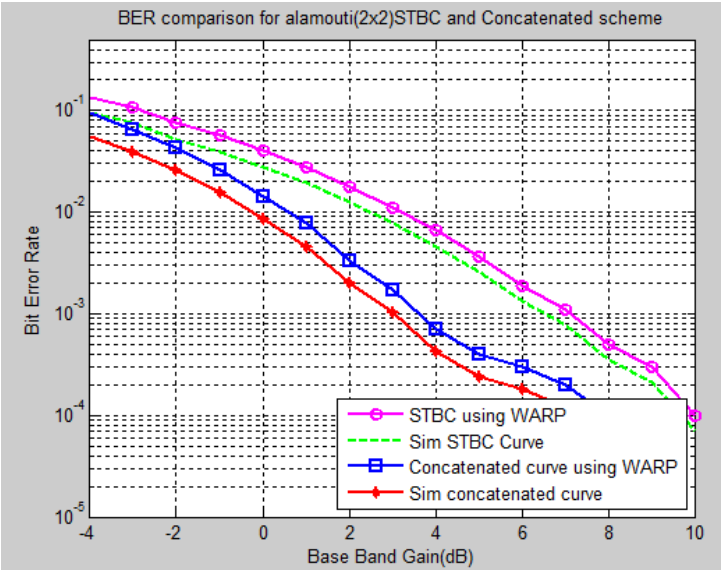

Figure 6.18 BER vs. SNR plot for 2x2 System

The modulation technique used is BPSK. From the experiments carried out we showed that for the transmission of same data using concatenated scheme can achieve a significant performance improvement in terms of bit error rate in comparison to the case when data is transmitted using only STBC. Implemented results shows that at a BER of 10^{-2} the concatenated scheme provides an improvement in SNR of 2.5dB over STBC scheme for 2x2 system. For the same value of BER the concatenated scheme provides an improvement in SNR of 2dB over STBC scheme for 2x1 system.

Conclusion

In this report the comparison among various performance metrics like BER, PSNR and Q-index has been done for various modulation techniques used for grey scale image transmission. For each modulation technique three different configurations are used i.e. 1x1, 2x1, 2x2. From the results it is concluded that when a grey scale image is transmitted using BPSK modulation the best results are obtained in terms of BER, PSNR and Q-Index. As we move from lower order modulation to higher order modulation the results are degrading for M-PSK modulation. The results obtained from WARP test bed shows that when the image is transmitted using 1x1 system the minimum acceptable value of PSNR is obtained at SNR of 9 dB, for 2x1 system the same value is obtained at 6 dB and for 2x2 system the same value is obtained at SNR of 4 dB for BPSK modulation. As we move to higher order modulation i.e. 4-PSK then with 1x1 system the minimum acceptable value of PSNR is obtained at SNR of 18 dB, for 2x1 system the same value is obtained at 16 dB and for 2x2 system the same value is obtained at SNR of 15 dB. It means as we move from 2-PSK to 4-PSK keeping all the others parameters same the minimum value of PSNR is obtained at small value of base band gain for 2-PSK and best results are obtained for 2x2 BPSK system. The results obtained from WARP test bed shows that when the image is transmitted using 1x1 system the minimum acceptable value of PSNR is obtained at SNR of 9 dB, for 2x1 system the same value is obtained at 6 dB and for 2x2 system the same value is obtained at SNR of 4 dB for 2-QAM modulation. As we move to higher order modulation i.e. 4-QAM then with 1x1 system the minimum acceptable value of PSNR is obtained at SNR of 15 dB, for 2x1 system the same value is obtained at 14 dB and for 2x2 system the same value is obtained at SNR of 13 dB. It means as we move from 2-QAM to 4-QAM keeping all the others parameters same the minimum value of PSNR is obtained at small value of base band gain for 2-PSK and best results are obtained for 2x2 system. It is concluded from the results that as low order of modulation i.e. M=2 the results are same for both BPSK and QAM. But as we move to higher values of M the M-QAM performs better than M-PSK.

When channel coding is also used with these 3 different configurations (1x1, 2x1, 2x2) for the transmission of mage then results obtained in terms of BER is better as compared to same 3systems (1x1, 2x1, 2x2) without channel coding.

Future Scope

Image transmission with different modulation techniques has been done using WARP test board. In future this work can be extended by transmitting video along with different channel coding techniques.

References

[1] J .Sifakis and S.Tripakis, "Building models of real time systems for application software," *Procedings of IEEE*, pp.100-102, January 2003.

[2] M.A.Hannan and A.Hussain, "Bit error rate for modulation scheme using Software Defined Radio," *IEEE conference on Electrical Engineering and Informatics*, pp. 445-446, 2009.

[3] Jose A. Garcia-Naya, David Ramirez, Jose M. Torres-Royo et.al, "Performance of STBC with real data," *16th IST on Mobile and Wireless Communications Summit*, pp.1-5, July 2007.

[4] J Dowle, S.H. Kuo, K. Mehrotra, I.V. McLoughlin, "An FPGA-Based MIMO and Space-Time Processing Platform," *EURASIP Journal on Applied Signal Processing*, vol. 2006, Article ID 34653, pp. 1-14, 2006.

[5] T. Kaiser, A. Bourdoux, M. Rupp, U. Heute, "Implementation Aspects and Test beds for MIMO systems," *EURASIP Journal on Applied Signal Processing*, vol. 2006, Article ID 69217, pp. 1-3, 2006.

[6] S.M.Alamouti,"A simple Transmit Diversity Technique for Wireless communications" , *IEEE journal on select Areas in Communications*, vol. 16, no. 8, pp. 1451-1458, October 1998.

[7] Chris Dick, Patric Murphy, J. Patric Frantz, "An FPGA implementation of Alamouti's Transmit Diversity Technique," *http://www. koala.ece.rice.edu/pubs/Mur2003Oct5AnFPGAImp.pdf*, March 12, 2012.

[8] Z.Wang and A.C. Bovik, "A universal image quality index," *IEEE Signal Processing Letters*, vol. 9, no. 3, pp. 81-84 March 2002.

[9] Duan Jinghong, Deng Yaling Liang Kun, "Development of Image processing System Based on DSP and FPGA," *International Conference on Electronic Measurements and Instruments*, pp. 2-791-2-794, October 2007.

[10] V. Roman, K.R. Namuduri, "Combined Source- Channel Diversity Scheme for Image Transmission over Wireless Channels," *IEEE International Conference on Communications*, pp.1219 – 1223, May 2005.

[11] Xiang Nian Zeng, A. Ghrayeb, "Performance Analysis of Combined Convolutional Coding and Space-Time Block Coding with Antenna Selection," *IEEE Global Telecommunications Conference*, pp. 795 – 799, November 2004.

[12] U.K. Kumar, B.S. Umashankar, "Improved Hamming Code for Error Detection and Correction," *2nd International Symposium on Wireless Pervasive Computing*, February 2007.

[13] Xuejing Zhang, Lin Xue, Jinping Li, "Software implementation of co-decoding algorithm of Hamming Codes," *International Conference on Computer and Communications Security*, pp. 107 – 110, December 2009.

[14] S.S. Sarnin, N. Kadri, A.M. Mozi, N.A. Wahab & N.F. Naim, "Performance Analysis of BPSK and QPSK Using Error Correcting Code through AWGN," *International Conference on Networking and Information Technology*, pp. 178-182, June 2010.

[15] R.B. Ertel & P. Cardieri, "Overview of Spatial Channel Models for Antenna Array Communication Systems," *IEEE personal Communication*, vol. 5, no. 1, pp. 10-22, February 1998.

[16] D. B. Smith and T. D. Abhayapala, "Bit-Error-Rate (BER) for modulation technique using Software defined Radio," *International Conference on Electrical Engineering and Informatics*, pp. 445 – 447, August 2009.

[17] Yair Linn, "A New Architecture for Coherent M-PSK Receivers," *IEEE International conference on Microwave Communications, Antennas and Electronics Systems*, pp 1-3, November 2009.

[18] Mostafa Wasiuddin Numan, Mohammad Tariqul Islam and Norbahiah Misran, "Implementation of Alamouti Encoder Using FPGA for MIMO Testbed," *International Conference on Advanced Computer Control*, pp. 188 – 192, January 2009.

[19] M.T. Islam, M.W. Numan, N. Misran, "Design and implementation of Alamouti encoder for 4G wireless system," *IEEE EUROCON 2009*, pp. 1676 – 1680, May 2009.

[20] Simon Haene, David Perels, and Andreas Burg, "A Real-Time MIMO Transceiver System Design, FPGA Implementation, and Characterization," *IEEE Journal on Selected Areas in Communications*, vol. 26, no. 6, pp. 877 – 889, August 2008.

[21] H.K. Mecklai and R.S Blum, "Transmit antenna diversity for wireless communications," *IEEE International Conference on Gateway to Globalization*, pp. 1500 – 1504, June 1995.

[22] Adrian Tarniceriu, Bogdan lordache, Silvian Spiridon, "An Analysis on Digital Modulation Techniques for Software Defined Radio Applications," *Proceedings of Semiconductor Conference*, pp. 571 – 574, September 2007.

[23] Feng Ge and Charles W. Bostian, "SDR Implementation Issues: Rf Front End Nonlinearity and Dynamic Computing Resource Allocation," *Proceedings of the SDR'09 Technical Conference and Product Exposition,* pp. 312-315, {month} 2009.

[24] Chris H. Dick and San Jose, "Design and Implementation of High-Performance FPGA Signal Processing Datapaths for Software Defined Radios" *http://.www.vmecritical.com/articles/id/?1664,* January, 2012.

[25] S. Wiess, A. Shligersky, S. Abendroth et.al, "Software Defined Radio Testbed Implementation," *http://www.eprints.ecs.soton.ac.uk/8275/1/IEEclq03_sdr.pdf*, January 10, 2012.

[26] S. Glass, V. Muthukkumarasamy and M. Portmann, "A Software-Defined Radio Receiver for APCO Project 25 Signals," *http://portal.acm.org/citation.cfm?id=1582395,* January 10, 2012.

[27] Junruo Zhang, Y.V. Zakharov, R.N. Khal, "Optimal detection for STBC MIMO systems in spatially correlated Rayleigh fast fading channels with imperfect channel estimation," *Conference Record of the Forty-Third Asilomar Conference on Signals, Systems and Computers*, pp. 1387 – 1391, November 2009.

[28] Lihua Yang, Bingke Yang, Guangliang Ren, Zhiliang Qiu, "Improved STBC transmit diversity scheme in high speed mobile environment," *IEEE International Conference on Communication Technology*, pp. 797 – 800, November 2010.

[29] Vahid Tarokh, Hamid Jafarkhani, and A. Robert Calderbank, "Space–Time Block Coding for Wireless Communications: Performance Results," *IEEE journal on Selected Areas in Communications*, vol. 17, pp. 451 – 460, March 1999.

[30] M.P.Fitz, J.Grimm, J.V.Krogmeier, "Results on code design for transmitter diversity in fading," *IEEE International Symposium on Information Theory*, July 1997.

[31] R. Ayoubi, J.P. Dubois, O. Abdul-Latif, "FPGA Implementation of a Novel Receiver Diversity Combining Technique for Wireless SIMO Systems," *IEEE*

International Conference on Signal Processing and Communications, pp. 37 – 40, November 2007.

[32] H. Dreizen, "Content-Driven Progressive Transmission of Grey-Scale Images," *IEEE Transactions on Communications*, vol. 35, pp. 289 – 296, March 1987.

[33] A. Hore, D. Ziou, "Image Quality Metrics: PSNR vs. SSIM," *20th International Conference on Pattern Recognition*, pp. 2366 – 2369, August 2010.

[34] Tolga M. Duman and Ali Ghrayeb, "coding for MIMO communication system", John Wiley & Sons, 2007," *http://www.ursi.org/Proceedings/ProcGA05/pdf/C08.1 (01584).pdf*, May 12, 2012.

[35] Martin and Christ, "MIMO Channel Characterization and Joint Channel Estimation and Detection in Digital Communications" *http://www.ee.kth.se/php/modules/publications/.../TRITA-S3-SB-0233.pdf, May 22, 2012.*

[36] S. Caban, C. Mehlfuhrer, L.W. Mayer, M. Rupp, "2x2 MIMO at Variable Antenna Distances," *IEEE Vehicular Technology Conference*, pp.1311 – 1315, May 2008.

[37] J.W. Wallace, "A real-time multiple antenna element testbed for; MIMO algorithm development and assessment," *IEEE Antennas and Propagation Society International Symposium*, vol. 2, pp.1716 – 1719, June 2004.

[38] "Addressing the Test Challenges of MIMO Communications Systems," *http://www.ni.com/white-paper/5689/en, May 23, 2012.*

[39] *Zhu Xiangbin, "Support QOS in Open Real Time Systems," International conference on computer science and software engineering, vol. 2, pp. 190-193, December 2008.*

[40] G. D. Durgin, *Space-Time Wireless Channels*, UpperSaddle River, NJ: Prentice Hall, 2003.

[41] E. G. Larsson, P. Stoica, *Space Time Block Coding for Wireless Communications*, Cambridge, UK: Cambridge University Press, 2003.

[42] Andrea Goldsmith, "Wireless Communication", Cambridge University Press, 2005.